

**UNIVERSITY OF VAASA**

**FACULTY OF TECHNOLOGY**

**ELECTRICAL AND ENERGY ENGINEERING**

Atte Hietalahti

**COMPATIBILITY OF TRADITIONAL EARTH FAULT PROTECTION  
FUNCTIONS FOR LONG CABLE FEEDERS IN COMPENSATED NET-  
WORKS**

Master's Thesis for the degree of Master of Science in Technology submitted for in-  
spection, Vaasa 20.05.2010

Instructor and Supervisor

Kimmo Kauhaniemi

Evaluator

Timo Vekara

## PREFACE

The subject for this thesis rose up from the engineering thesis completed at the end of 2006. I was asking for the subject for my master's thesis at beginning of 2007. *Aimo Latvala* from ABB Substation automation gave me the idea of far going investigations of results of previously submitted engineering thesis. I was advised that subject would not be the easiest one. Usually I have set my goals high, so it was directly clear that I would be ready for the challenging work and I took the job.

During the work it was not obvious all the time, am I going to cope with the thesis. Regardless the hard times, I every time I got up and fought back to walk the line. I would like to thank all the people who have supported me during the work, especially the people in ABB Substation Automation who have been patient to wait me to complete the work. *Aimo Latvala*, you gave me the spirit to believe that this is not a rocket science. *Janne Altonen* and *Ari Wahlroos*, you gave me the best information of distribution network faults what man could get. Big thanks go to the University of Vaasa's Fabriikki buildings room F640. *Kimmo Kauhaniemi*, you guided through this project with determined role of supervisor. I had a feeling that every time I had problems it was fine to come to ask for help. Thanks go also to boys of electrical engineering's project room. It has been pleasant to come there every day. Thanks for tolerating my talks about cars and other dummy stuff. It was easier for me that I was allowed to listen to Johnny Cash every day.

And finally I would like thank my family and *Johanna* for their support. When I felt bad with this workload, you cheered me up and believed that someday I'm going to be the Master of Science in technology.

Laihia 14.05.2010

Atte Hietalahti

## TABLE OF CONTENTS

PREFACE	2
LIST OF SYMBOLS AND ABBREVIATIONS	5
ABSTRACT	8
1. INTRODUCTION	10
2. BASIC THEORY OF THE THREE-PHASE NETWORK	13
2.1. Distribution network	13
2.1.1. Network configurations	13
2.1.2. Normal use of different network structures	15
2.2. Conductor types	18
2.2.1. Overhead lines	19
2.2.2. Underground cables	22
2.3. Methods to ground the network	23
2.3.1. Isolated network	23
2.3.2. Resistance earthed network	24
2.3.3. Directly earthed network	24
2.3.4. Compensated network	24
3. FUNDAMENTALS OF NETWORKS FAULT SITUATIONS	28
3.1. Faults concept	28
3.1.1. Symmetrical faults	28
3.1.2. Asymmetrical faults	28
3.2. Basic theory and data of earth faults	29
3.3. Basic measurements at the fault situation	30
3.4. Earth fault in the compensated network	31
3.5. Equation to determine size of compensation coil	33
3.6. Introduction to symmetrical components	34
4. EARTH FAULT PROTECTION	38
4.1. Microprocessor-based relay	38
4.2. Operational characteristics	39
4.3. Elements of the protection system	42
4.3.1. Instrument transformers and sensors	42
4.3.2. Earth fault current compensation equipment	44
4.4. Protection methods	45
4.4.1. Base angle criterion	46
4.4.2. $I_0 \cos(\varphi)$ protection method	47
4.4.3. Wattmetric protection method	47
4.4.4. Neutral admittance protection method	48

5.	DISTRIBUTION NETWORK TO BE STUDIED	49
5.1.	Network parameters	49
5.2.	Network modeled by PSCAD	54
5.3.	Matlab® script	57
6.	SIMULATIONS	59
6.1.	Verification of the non-linear increase of resistive fault current as a function of cable length	59
6.2.	Base angle criterion	61
6.3.	$I_0\cos(\varphi)$ protection method	67
6.4.	Wattmetric protection method	70
6.5.	Neutral admittance protection method	73
6.6.	Odd behaviour of zero sequence current when fault is at the end of the feeder	78
7.	CONCLUSIONS	81
7.1.	Base angle criterion	81
7.2.	$I_0\cos(\varphi)$ protection method	82
7.3.	Wattmetric protection method	82
7.4.	Neutral admittance protection method	83
	REFERENCES	84
	APPENDICES	
	Appendix 1. Matlab® script to import PSCAD results to Matlab®	88
	Appendix 2. Data table of PSCAD simulations	90

## LIST OF SYMBOLS AND ABBREVIATIONS

*SYMBOLS*

$\omega$	Angular frequency
$\varphi$	Phase angle
$a$	Phase shifting operator
$A$	Symmetrical transformation matrix
$A^{-1}$	Inversed symmetrical transformation matrix
$\text{adj}(A)$	Adjugate of matrix A
$B$	Susceptance
$C$	Capacitance
$C_0$	Earth capacitance per phase
$\text{det}(A)$	Determinant of matrix A
$E$	Voltage source
$F_i$	Current error
$G$	Conductance
$I$	Current
$I_{\text{bgnw}}$	Earth fault current of the background network
$I_{0\text{dft}}$	Zero sequence current, which is driven through Discrete Fourier Transform (DFT) to get the zero sequence current phasor
$\underline{I}_C$	Current through earth capacitance
$I_{\text{Ctot}}$	Total uncompensated earth fault current of the network at the zero resistance fault
$\underline{I}_{\text{ef}}$	Magnitude of earth fault current
$\underline{I}_f$	Fault current
$\underline{I}_L$	Current through Petersen coil
$I_p$	Rms current of transformers primary coil
$\underline{I}_{R+}, \underline{I}_{S+}, \underline{I}_{T+}$	Phase R, S, T positive sequence current
$\underline{I}_{R-}, \underline{I}_{S-}, \underline{I}_{T-}$	Phase R, S, T negative sequence current
$\underline{I}_{R_p}$	Current through Peteresen coil's parallel resistance
$\underline{I}_{R_l}$	Current through leakage resistance
$I_s$	Rms current of transformers secondary coil
$j$	Imaginary unit
$k$	Compensation degree
$K_n$	Transformers transformation ratio

$l$	Length
$L$	Inductance
$R$	Resistance
$R_0$	Zero sequence resistance
$R_1$	Leakage resistance
$R_f$	Earth fault resistance
$R_L$	Petersen coils parallel resistance
$R_p$	Grounding resistance
$\underline{U}_0$	Zero sequence voltage
$U_0$	Magnitude of zero sequence voltage
$U_{0\text{dft}}$	Zero sequence voltage, which is driven through Discrete Fourier Transform (DFT) to get the zero sequence current phasor.
$\underline{U}_+$	Positive sequence voltage
$\underline{U}_-$	Negative sequence voltage
$U_p$	Magnitude of primary voltage
$\underline{U}_{R0}, \underline{U}_{S0}, \underline{U}_{T0}$	Phase R, S, T zero sequence voltage
$\underline{U}_{R+}, \underline{U}_{S+}, \underline{U}_{T+}$	Phase R, S, T positive sequence voltage
$\underline{U}_{R-}, \underline{U}_{S-}, \underline{U}_{T-}$	Phase R negative sequence voltage
$\underline{U}_s$	Neutral point voltage
$\underline{V}_p$	Phase voltage vector
$\underline{V}_s$	Symmetrical voltage vector
$X_0$	Zero sequence reactance
$X_C$	Capacitive reactance
$X_L$	Inductive reactance
$\underline{Y}$	Admittance
$\underline{Z}_0$	Zero sequence impedance
$\underline{Z}_+$	Positive sequence impedance
$\underline{Z}_-$	Negative sequence impedance
$\underline{Z}_N$	Ground impedance
$\underline{Z}_f$	Fault impedance

*ABBREVIATIONS*

ABB	Asea Brown Boveri
ACSR	Aluminium conductor, steel reinforced
comp	Compensation degree
bg network	Back ground network
DC	Direct current
EMTDC	EMTDC is an electro-magnetic transient simulation engine, which uses PSCAD as a graphical user interface. EMTDC is a trademark of Manitoba Hydro.
HV	High voltage
HVDC	High voltage direct current
LV	Low voltage
MV	Medium voltage
nbgwvf	Number of background network feeders
pi sec	PSCAD block of transmission line
length	Length of studied feeder
location	Fault location
PSCAD	Power system computer aided design. PSCAD is the graphical user interface for electro-magnetic transients simulation engine EMTDC. PSCAD is a registered trademark of Manitoba HVDC Research Centre Inc.
RC-Circuit	Electrical filter circuit containing resistance and capacitance.
rms	Root mean square
XLPE	Polyethylene

---

**VAASAN YLIOPISTO****Teknillinen tiedekunta****Tekijä:**

Atte Hietalahti

**Diplomityön nimi:**

Nykyisten maasulkusuojausmenetelmien soveltuvuus laajojen kompensoitujen kaapeliverkkojen suojaukseen.

**Valvojan nimi:**

Professori Kimmo Kauhaniemi

**Ohjaajan nimi:**

Professori Kimmo Kauhaniemi

**Tarkastajan nimi:**

Professori Timo Vekara

**Tutkinto:**

Diplomi-insinööri

**Oppiaine:**

Sähkötekniikka

**Opintojen aloitusvuosi:**

2003

**Diplomityön valmistumisvuosi:**

2010

**Sivumäärä: 87 (94 liitteinen)**

---

**TIIVISTELMÄ**

Gudrun myrsky iski eteläiseen Ruotsiin tammikuussa 2005. Myrsky tuhosi ja vaurioitti yli 20 000 kilometriä jakeluverkkoa. Seurauksena myrskystä ja uusien lakien seurauksena jakeluverkkoyhtiöiden tuli vastata sähkön jakelun uusiin vaatimuksiin. Täten useat verkkoyhtiöt Ruotsissa päättivät muuttaa avojohtoverkkoja maakaapeliverkoiksi parantaakseen verkkojen käytettävyyttä. Tämän seurauksena keskijänniteverkkorakenne muuttuu selvästi kaapeliverkkopainotteiseksi, joissa yksittäisten johtolähtöjen pituudet saattavat nousta jopa kymmeniin kilometreihin. Maakaapelin käyttö nostaa merkittävästi verkon kapasitiivista maasulkuvirtaa. Lisäksi se aiheuttaa laajoissa säteittäisverkoissa myös selkeän resistiivisen virran kasvun. Yleisesti ottaen kasvanut resistiivinen virta aiheuttaa haasteita maasulkusuojaukselle, koska sitä ei pysty kapasitiivisen tehon tapaan kompensoimaan pois.

Tämän työn tarkoituksena on tutkia perinteisten moderneissa suojareleissä olevien maasulkusuojamenetelmien toimivuutta. Tutkimukset tehdään 10 kV:n kompensoidussa verkossa, jossa esiintyy suuri resistiivinen vikavirta. Nämä mittausmenetelmät ovat peruskulma-asettelu, Icos( $\varphi$ ) ja Wattmetric menetelmät. Lisäksi mukana on harvinaisempi admittanssiin perustuva suojausmenetelmä. Kaikkia menetelmiä tutkitaan erikseen ja niiden sopivuus tutkimusongelmaan tutkitaan. Tämä arviointi perustuu yleistä suorituskykyä mittaaviin asioihin kuten selektiivisyyteen, herkkyyteen, asetusten soveltavuuteen ja mahdollisuuksiin muokata erilaisiin muuttuviin verkkomalleihin.

Työn aikana tehdyt simuloinnit osoittivat, että kaikki perinteiset maasulkusuojausmenetelmät suoriutuvat tehtävästään kohtuullisen hyvin. Paremmuusjärjestyksessä menetelmät ovat admittanssimenetelmä, Wattmetric, Icos( $\varphi$ )- ja peruskulma-asettelu. Admittanssimenetelmän paremmuus selittyy sen kyvyllä systemaattisesti havaita maasulku ja joustavuudella soveltua eripituisiin johtolähtöihin.

---

**AVAINSANAT:** Kompensoitu verkko, symmetriset komponentit, keskitetty kompensointi, maasulku, maasulkusuojaus, laaja kaapeliverkko ja resistiivinen vikavirtakomponentti.



---

**UNIVERSITY OF VAASA****Faculty of technology**

<b>Author:</b>	Atte Hietalahti
<b>Topic of the Thesis:</b>	Compatibility of traditional earth fault protection functions for long cable feeders in compensated networks.
<b>Supervisor:</b>	Professor Kimmo Kauhaniemi
<b>Instructor:</b>	Professor Kimmo Kauhaniemi
<b>Evaluator:</b>	Professor Timo Vekara
<b>Degree:</b>	Master of Science in Technology
<b>Major of Subject:</b>	Electrical Engineering
<b>Year of Entering the University:</b>	2003
<b>Year of Completing the Thesis:</b>	2010

**Pages: 87 (94 with Appendices)**

---

**ABSTRACT**

In January 2005, the storm Gudrun hit the south of Sweden. More than 20 000 kilometers of distribution lines were damaged during the storm. As a result of the Gudrun experience and forced by the new compensation regulations, the distribution network owners had to answer to new demands of electrical distribution. Several of them in Sweden plan to, during a near future, replace numerous of rural overhead lines by underground cables. As a consequence of this development, HV to MV-substations will consist of more and more of large cable networks, where individual cable feeders can be tens of kilometers long. The extensive use of underground cable involves significant increase of the capacitive earth fault current. In networks with long radial cable feeders, this also leads to increased active losses, as the active earth fault current contribution drastically increases. Generally, the increased resistive component makes the management of earth faults more difficult because this component cannot be directly compensated like the capacitive component.

The primary aim of the thesis is to investigate the performance of the traditional protection functions, which are available in modern feeder protection relays and terminals. Investigations will be run in 10 kV compensated networks with large resistive earth fault current component. These protection functions include phase angle criterion-,  $I_{\cos(\varphi)}$ - and Wattmetric-functions. As a novel earth-fault protection function, neutral admittance- based earth fault protection is also included in the study. Each protection method is studied separately, and its suitability to this application is evaluated. This evaluation is based on performance considerations such as overall selectivity, sensitivity, suitability of settings and their ranges, and the effect of network changes on the directly compensated networks.

During the simulations, all protection functions showed rather good performance. In the ranking, the best method was neutral admittance, then Wattmetric,  $I_{\cos(\varphi)}$ - and base angle criterion. Superiority of the admittance method is explained by its systematical way to identify earth fault and flexibility for different feeder lengths.

---

**KEYWORDS:** Compensated network, symmetrical components, centralized compensation, earth fault, earth fault protection, long cable feeder and resistive component of earth fault current.

## 1. INTRODUCTION

In this thesis a compensated medium voltage cable network is studied. The network is compensated using inductances and earthing resistances in parallel connection. The study is focused to the earth faults occurring in a feeder with a length up to the 56 km.

The need for this thesis has come up during the year 2005. At that time storm Gudrun hit through southern Sweden. The force of the storm was unexpected, although, before entering Sweden it had already damaged badly Danish nature severely, and electrical distribution network. In the storm, the rural areas suffered more than the urban areas: During the one night storm, 17 human lives were lost and money costs accounted to somewhere between 360 to 450 millions of Euros. The estimation is based to the Swedish crown exchange rate at January of 2005. These huge losses forced Swedish government to enact new law how medium voltage network should be built in the future. This law included for example maximum rating of the existing earth fault current and guidelines how network should be prepared against adverse conditions. In the most cases this marked end to the common way to build medium voltage networks by overhead lines. (French ministry of environment 2005; Carpenter 2005; Regeringskansliet 2005)

In the new long cable networks it has been shown that some new challenges occur when traditional protection procedures are used. Challenges arise when higher feeder lengths are tried to be protected against earth faults. The problem is caused by the resistive component of fault current. Up to this day, it has been assumed that resistive current will increase in a linear fashion with the feeder length. In their publications first Lars Andersson (2005: 13) and then Jussi-Pekka Pouttu (2007b) have noticed the increase of resistive fault current is not linear. Today, at the commonly used protection functions, the non-linear increase of resistive current is not taken into account.

The main purpose of this thesis is to investigate the performance of the traditional earth fault protection schemes, which are available in modern feeder protection relays and terminals. Investigations are carried out in compensated medium voltage network with long cable feeders. The performance of each protection method is evaluated utilizing computer simulations.

These simulations are carried out with the PSCAD electrical network simulation program and the Matlab® calculator program. First the electrical network is modeled with PSCAD, and then that output data is processed with Matlab® to get the desired output data. Short presentations of both programs are given below.

Originally the PSCAD program was an answer for an urgent need to simulate Nelson rivers HVDC system at Manitoba, Canada in 1970's. During the simulations, the program showed its potential and the development continued over the next two decades. First commercial version of PSCAD was published in 1993 for the UNIX platform. Current version of the program is published in 2007 and version number is 4.2.1. This version is also used during the simulations of this thesis. The program is originally designed to simulate electromagnetic transients of networks, but also steady-state values can be easily acquired. The user interface of PSCAD provides efficient circuit schematics construction solutions, the integrated graphical result displays and information output channel to txt file. (PSCAD 2010a, 2010b)

Matlab® is a product family of MathWorks. Commercially Matlab® came available in the 1980's, but the first code lines of the program were written in the 1970's. Cleve Moler has written the original code. First Matlab® was a solution for students to access other programs without learning FORTRAN, but in 1983 the potential of the program was discovered. It was rewritten by C language by Jack Little and it came commercially available. Commonly, the term Matlab® describes a computer program which allows users to powerfully solve different types of mathematical problems. The user interface of Matlab® gives the user tools from typical command prompt commands to highly developed graphic modelling and powerful problem solving solutions. (MATLAB 2010)

This thesis is divided to four sections. The first section describes the three-phase network in general. Then the basic fault situations are presented. The second part of the thesis focuses to earth fault protection. Examples of earth fault calculations are given and a mathematical calculation method called symmetrical components is presented. The third part of the thesis presents the studied network with its parameters. The fourth and the last part of the thesis present simulation results made in the studied network.

Results from different protection methods will be shown in detail and finally their performance will be analyzed.

## 2. BASIC THEORY OF THE THREE-PHASE NETWORK

### 2.1. Distribution network

Normally, distribution networks are graded by used voltage. Voltage levels high, medium and low are normally used. Abbreviations HV, MV and LV are typically used. HV level is voltage above 35 kV, MV is between 5 kV to 35 kV and LV is above this level. Voltage levels are used in the order where level is lowest at the customer end. By doing so, power losses are minimal and voltage at the customer level is less dangerous. A basic function of distribution network is to deliver electrical power to customers without interruptions. The most vulnerable parts of distribution network are located in the rural areas. To avoid fatal situations, voltage levels at these areas are medium or low. (Lakervi 2006: 2)

#### 2.1.1. Network configurations

Typical distribution network is built in one of the following configurations. These configurations are radial network, open ring network, link arrangement system, closed ring network, satellite network and primary network system. Every configuration has its benefits and drawbacks.

Radial network is the cheapest and usually also the most unreliable distribution system available. Configuration is based on single trunk lines going to different directions from the substation. If a fault occurs at the line, the whole line has to be turned off. The reliability can be improved by adding remote controlled feeder disconnectors along the line. By doing so, faulty end of line can be removed from the distribution system.

Open ring network is a little more reliable configuration than the radial network. In the open ring network, there is a possibility to connect one or more radial networks together during a fault situation with remote controlled disconnectors. By doing so, back-up feed to the healthy part of the network can be provided. By adding more than one disconnec-

tor to the same ring, the network achieves even more reliability. It is then much more likely that only the majority of the faults will affect a small part of the network.

Link arrangement system network is a modified open ring network. If there is a fault at open ring network substation's busbar, the whole open ring network is going to fail. By connecting the open ring network between multiple substations, the failure in one substation won't cause the whole network to fail. By doing so, outage times can be reduced. Although the building costs are higher than in a normal open ring network, the link arrangement system is a good choice, when reliable and relatively cheap power feed is needed.

A still more developed configuration is the closed ring network. Disconnectors are replaced by circuit breakers. One sectionalizing circuit breaker is also added to separate faults. Use of closed ring network improves reliability by 50 % compared to the open ring network. Much better results have been gained, because relays are today micro-processor-based and remote use possibilities are today considerably better than they used to be.

A satellite network is a configuration, where one trunk line feeds multiple branch lines. At the branch lines there is a satellite transformer, which lowers the voltage to the customer end level. Line coupling is handled via breaker, which is equipped with a high voltage fuse. If some branch suffers a fault, it can be directly removed by using the fused breaker. Especially in Scandinavian satellite networks, power delivery costs are 8 – 15 percent lower than in traditional network configurations. The variation in cost is due to different housing methods.

Primary network system is a result of the three mentioned configurations. Closed ring, link arrangement system and radial network's good features are joined together. At this network, radial networks are connected from different ends to different substations. In the end, stations and radial networks form a ring. (Lågland 2004: 31 - 41)

### 2.1.2. Normal use of different network configurations

All of the above mentioned network configurations have their own properties. Due to these properties they suit to different conditions and are able to meet specified requirements. A short presentation of each configuration applied to its typical use, is given.

Normally, radial systems are used in the rural areas, where only few people live and the power consumption is pretty low. The configuration is pretty simple. This is a benefit, because this type of network is the cheapest configuration to set up. Drawback is that back-up feed cannot be naturally provided. The basic principle of radial network is shown in the figure 1.

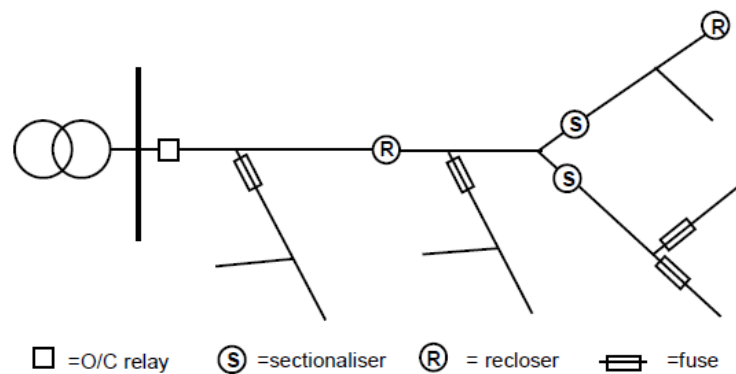


**Figure 1.** Example of a radial network. (Tarchini J & G Sandez 2003)

Open ring configuration is the most common way to build and connect cable networks. The construction investments of an open ring network are higher than those of a radial network, but they don't radically increase. The number of outages is roughly comparable to the radial network, but the outage durations are much shorter than in radial network. Open ring configuration is used on both rural and more crowded areas. The basic principle of open ring network is shown in the figure 2.

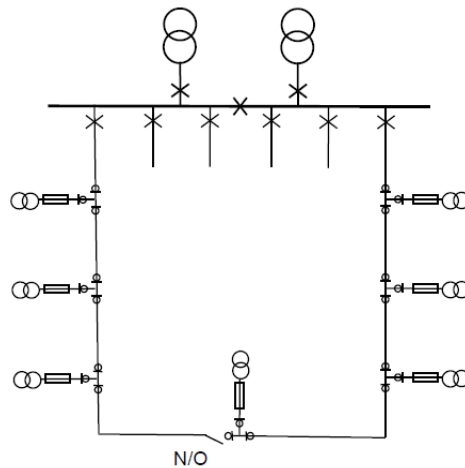


**Figure 2.** Example of an open ring network. At normal use sectionalizing circuit breaker is open. (Lågland 2004: 33)

In the link arrangement system, when radial feeders are connected to the more than one, substation, a more reliable power distribution can be provided. Typically, link arrangements systems are introduced in areas, where are many substations in a relatively small area. When new radial network is set up, it is usual to connect it from different ends to different substations. Normally, link arrangement system is applied to more crowded areas. The basic principle of link arrangement system network is shown in the figure 3.

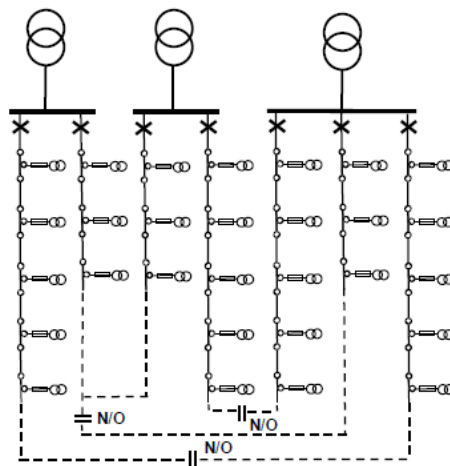


**Figure 3.** Example of a link arrangement system network. (Tsao 2003)



Closed ring network is the most expensive configuration available. Its reliability lies on the number of sectionalizers placed to the network. The more sectionalizers there are, the stronger the network is against distribution interruptions. Closed ring network is normally used in the urban areas, because of the high fault current. The shorter the cables are, the lower the fault current is. The closed ring network is the configuration of the future. The basic principle of closed ring network is shown in the figure 4.

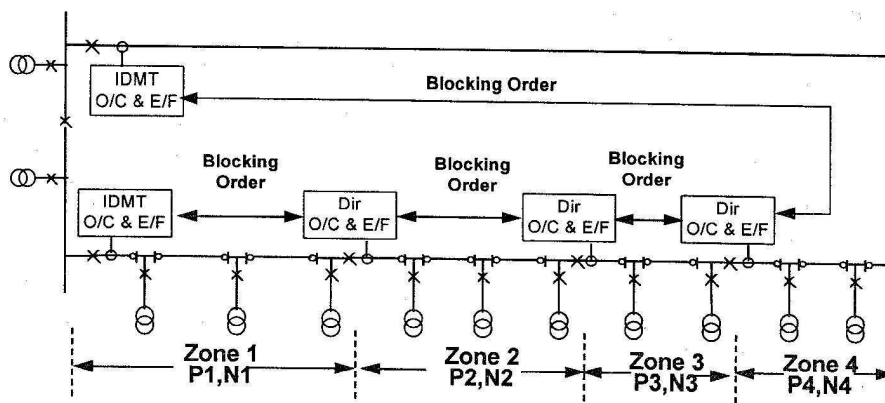


**Figure 4.** Example of a closed ring network. (Tobias 1998)

Satellite network is a typical configuration to be applied to urban area. The reason for this is that satellite transformers can be easily fitted to the existing infrastructure, because of their relatively small physical size. Satellite network's reliability is in the average level. The basic principle of satellite network is shown in the figure 5.

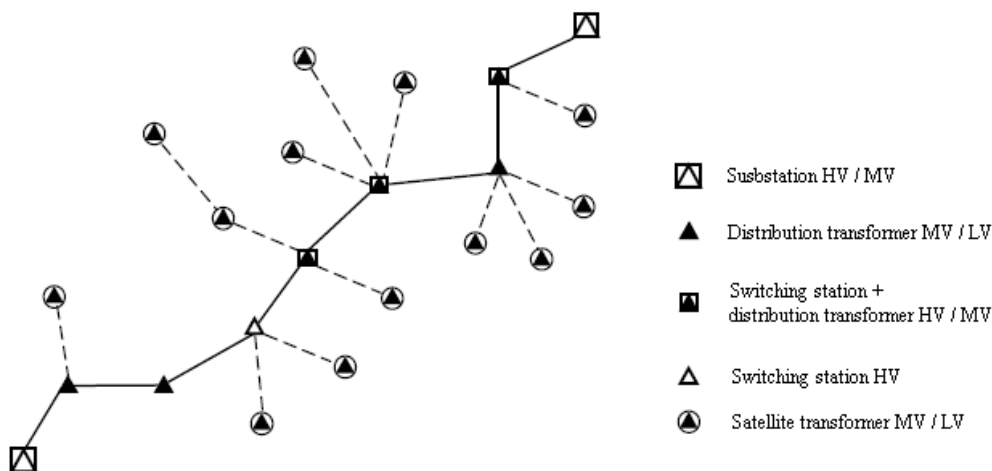


**Figure 5.** Example of a satellite network. (Naver J & R Stilling-Petersen)

A primary network system is the most reliable network system available. It relies on multiple back-up feeds provided by the configuration. The shorter the loops at the network are, the smaller the area of distribution interruption can be limited. Normally this network configuration is used in the urban areas. The basic principle of a primary network system is shown in the figure 6. (Lågland 2004: 31 - 41)

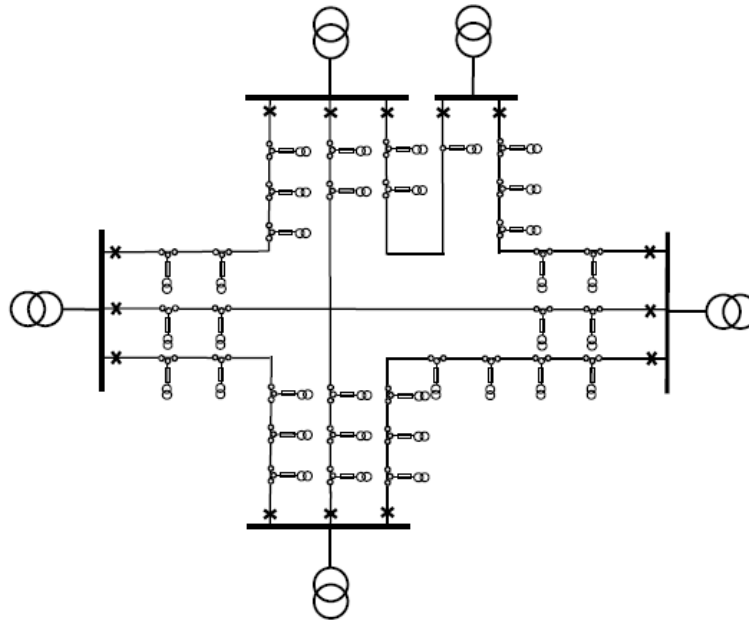


**Figure 6.** Example of primary network system. (Tsao 2003)

## 2.2. Conductor types

Typically there are two major ways to set up the distribution network: overhead lines and underground cables. The better conductor type depends a lot on the housing conditions of the area. In the countryside, overhead lines are commonly used, but in the urban area underground cable is normally a much better alternative. Normal percentage level of use of overhead lines in an individual country is 30 - 40 %. There are some exceptions: In the Far East and South America, it is really common to use overhead lines even in an urban area. For example overhead lines build 98 % of Pakistan's MV network. However, in areas where forces of nature are harsh, underground cables are commonly used to secure reliable power distribution. Both conductor types have their own benefits

and drawbacks and they are briefly introduced in the following two chapters. The essential amount of earth fault current produced by conductor can be calculated by equation

$$I_f = \sqrt{3}\omega C_0 U_p, \quad (1)$$

where  $I_f$  is magnitude fault current,  $\omega$  is angular frequency,  $C_0$  is earth capacitance per one kilometre and  $U_p$  is magnitude of line-to-line voltage. (ABB 2000: 248; Beaty 1998; Lågland 2004: 79 - 80)



**Figure 7.** Overhead lines in use at urban area in India.

### 2.2.1. Overhead lines

Overhead line is the most typical way to deliver electrical power to customers, but the rate of installing new overhead lines is decreasing. In overhead lines the conductor hangs from a tower by the help of an insulation bar. There are several types of towers and conductors. Typical span at the HV overhead line is ~400 meters and major limiting

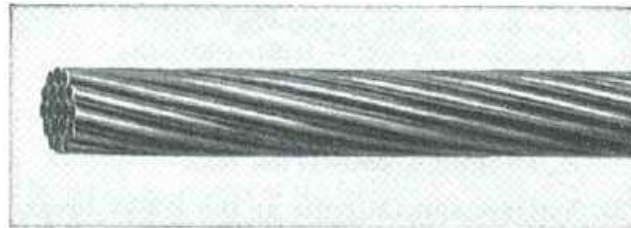
condition is the sag of the line. Naturally, in the MV network the span is shorter. (Weedy 1987: 110 - 111)



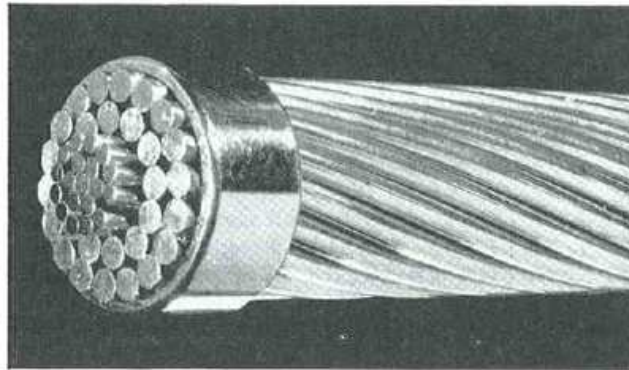
**Figure 8.** Typical tower type used in MV grid in Finland. (Turvatekniikan keskus 2007: 8)

Prevailing conductor types are stranded and hollow conductors. The use of stranded conductor is usually explained by better flexibility when compared to solid ones. When hollow conductors are used, material costs are lower, but a more important reason is the skin effect. Skin effect is a phenomenon where current flow packs to the skin of conductor. This problem is normally taken into account when the conductor is manufactured from strands, but also a hollow structure is used. There can also be two different materials together, like aluminium and steel. Use of composite materials has mostly the same benefits as the stranded and hollow conductors have, but they are achieved in another way. For example, in a flexible ACSR conductor there is more steel than aluminium,

but if conductivity needs to be increased, more aluminium is used. An earth fault current for typical overhead line conductor in a 20 kV network is estimated to be near 67 mA per km. When earth capacitance is known, it can be also calculated by utilizing the equation 1 on the page 19. In this work FEAL99 overhead line is used. (ABB 1997: 32 - 33; Lakervi & Partanen 2008: 186)



A typical stranded conductor, (bare copper).



A typical ACSR conductor.



A typical Anaconda Hollow Copper Conductor.

**Figure 9.** Different types of overhead line conductors. (ABB 1997: 32)

Benefits of overhead line include easy installation and maintenance. At the beginning of the lifespan of overhead line, it is a beneficial option if you compare it to the cable option. All of these reasons make it the normal choice in the developing countries even though the choice should be the opposite. The drawback of an overhead line is its resistance against harsh nature. For example, falling trees easily cause earth faults and in more severe conditions even break the wire. (Berlin, Hansson & Olofsson 2008)

### 2.2.2. Underground cables

The underground cable is a modern way to deliver electrical power to customers. Conductors are buried in the ground, by having conductor in the ground, the power delivery is considerable more reliable, because harmful weather conditions such as harsh wind cannot affect them. A landscape looks more natural as there are no towers on the ground and conductors hanging in the air. In a typical structure of three-phase underground cable, all three phase conductors are located inside the same sheath. The insulation material may vary, but technology is always roughly the same. For example, ABB is using XLPE (polyethylene) as an insulator, which can cover up all voltages up to 220 kV. (ABB 2008)



**Figure 10.** Different types of underground cables. (ABB 2008: 3)

Underground cable installation costs are higher than those of overhead lines, but this cost will be gained back via lower fault rate and longer life span. Nature's phenomena which occur in the atmosphere cannot break the conductor, but when ground is dug near the cable, it can easily be broken. Earth fault current for typical cable conductor in 20 kV network is estimated to be near 2,7 to 4 A per km. When earth fault capacitance toward earth is known, it can be also calculated by utilizing the equation 1 on the page 19. In this work AXCEL 3X95/16 cable is used. (Lakervi etc. 2008: 186)

### 2.3. Methods to ground the network

The grounding of network means connection of the neutral points of the power system to the ground. Normally in European MV distribution networks, there are four basic principles to ground the network: First alternative is to isolate the network from the ground. Second alternative is to connect the neutral points of the network to the ground through a resistor. Third alternative is to connect the neutral points of the network directly to the ground. The fourth alternative is to connect neutral points of network to the ground via reactance. A combination of reactance and resistance is often used. The choice between different methods depends on many technical and economical parameters. (ABB 1999: 137 – 140; Lågland 2004: 42)

#### 2.3.1. Isolated network

At the isolated, or on the other words unearthed, network; there is no connection to the ground from the system's neutral points. The earth fault within the isolated network causes only fault current through the network's earth capacitance. The conductor type, length of galvanically connected to the distribution network and line-to-line voltage; all effect on the amount of fault current. The main drawback of the isolated network is its ability to limit overvoltages. This grounding method is particularly used in areas, where grounding conditions are bad. For example, Finland is a country where isolated network is widely used. For a long cable network, isolation is not a good solution. As earth capacitance in a cable network is much bigger than in equal length overhead line network, earth fault current increases to too high levels. The drawback of isolated network is higher insulation costs than in other grounding methods. (Lågland 2004: 42 - 44)

#### 2.3.2. Resistance earthed network

When talking about resistance earthing, terms low and high are normally introduced. When using term low, a small resistance is installed to the network's neutral point's connections to the ground. This procedure is introduced at large MV distribution systems where capacitive fault current is so high that it has to be directly cleared. This relatively high earth fault current doesn't give good enough selectivity for the protection

relay. Resistance is usually introduced to increase fault current to help protection to be more selective. Normally the resistance is set to a level where current flowing through the resistor is 50 – 800 A. The most critical restricting factor in calculating the resistance is the distribution transformer's thermal durability. When the power feeder is a generator, not a transformer, higher resistance is often needed to avoid damage to the iron core of the generator in a fault situation. (Hakola & Lehtonen 1996: 22)

High resistance earthing is normally introduced in MV and LV industrial systems. High resistance earthing also provides pretty reliable power distribution, because during a single fault, power doesn't normally have to be shut down. Normally high resistance earthing can also be used in the public MV networks where capacitive earth fault current is not higher than a few tens of amperes. (Hakola etc. 1996: 21)

### 2.3.3. Directly earthed network

In directly earthed networks, the neutral point of the network is connected directly to the ground. When grounding is carried out in this way, overvoltages at the healthy phases are well limited during the faults. Drawback is that the earth fault current is as high as the short circuit current between two phases. Direct earthing is in use in networks where short circuit current is small. In North America's overhead line networks this is the most common way to make grounding. (Lågland 2004: 50)

### 2.3.4. Compensated network

At the networks where the capacitive fault current is big, the resulting fault current can be radically reduced by introducing inductance coil to the neutral point of the distribution system. Networks operating with this principle are called either compensated systems, Petersen coil earthed systems by the name of the inventor of this earthing method or resonant earthed systems. Appropriate size of the coil is calculated when size of the network's earth capacitance is known. The goal is to try to compensate most of capacitive current away. Normal level of compensation is near 100 %, but never exact. Exactly 100 % is not used, because a small amount of reactive current makes protection procedure easier.



Compensation degree of network can be calculated by utilizing equation

$$k = \frac{I_L}{I_{Ctot}}, \quad (2)$$

where  $k$  is compensation degree,  $I_L$  is magnitude of current through compensation coil and  $I_{Ctot}$  is magnitude of total uncompensated earth fault current of the network at zero resistance fault. Network can be driven as under- or over-compensated. In an under-compensated network, the fault current is capacitive and in an over-compensated inductive. The chosen compensation degree depends on lots of network parameters like type of conductor, length of the conductor and type of grounding method. The precise resonant earthing cannot be gained in reality, because of the natural asymmetry of the different phases. Usually, the resistor is placed in the parallel with the coil. This is carried out to make protection procedure more selective. (Hakola etc 1996: 16)

Earthing can be carried out via one big compensation device placed to the main feeder station, or by utilizing smaller devices placed to local feeder stations. Using one big compensation device is a very rigid and expensive procedure, but technically, relatively simple. Centralized compensation is often used, when earthing conditions are poor and network's earth fault current is higher than 35 A. Compensators can have tuneable or fixed inductance value. It can be controlled locally or remotely. The example of centrally compensated is shown in figure 11. (Pouttu 2007a: 29 – 31; Achleitner, Fickert, Obkirche & Sakulin 2007)

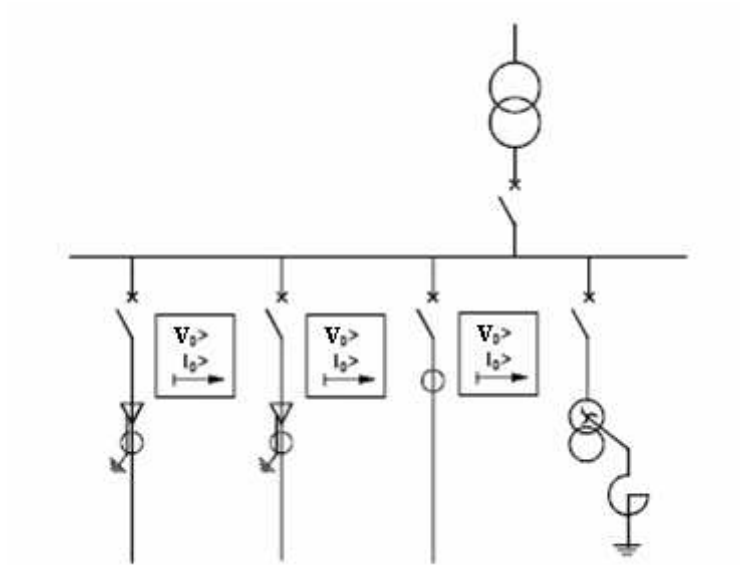


**Figure 11.** Centralized compensation at MV network. (Pouttu 2007a: 30)

Decentralized compensation is used in rapidly growing networks. It's a cheap solution when compared to centralized compensation. It's normally used when earth fault current is from 20 to 30 A. In an earth fault situation, every small compensator connects parallel. When zero sequence voltage  $\underline{U}_0$  is same in every part of the network, it creates inductive current to the compensator, and this way compensates capacitive current away from the network. Decentralized compensation can be used even in a network which is already centrally compensated. When it seems that a big compensation device has been adjusted to the limit, it's still possible expand the grid. In this situation it needs to be taken care of that compensation degree of the new part of network is set to be equal with old part of the network. The example of decentrally compensated is shown in figure 12. (Pouttu 2007a: 29 - 31)

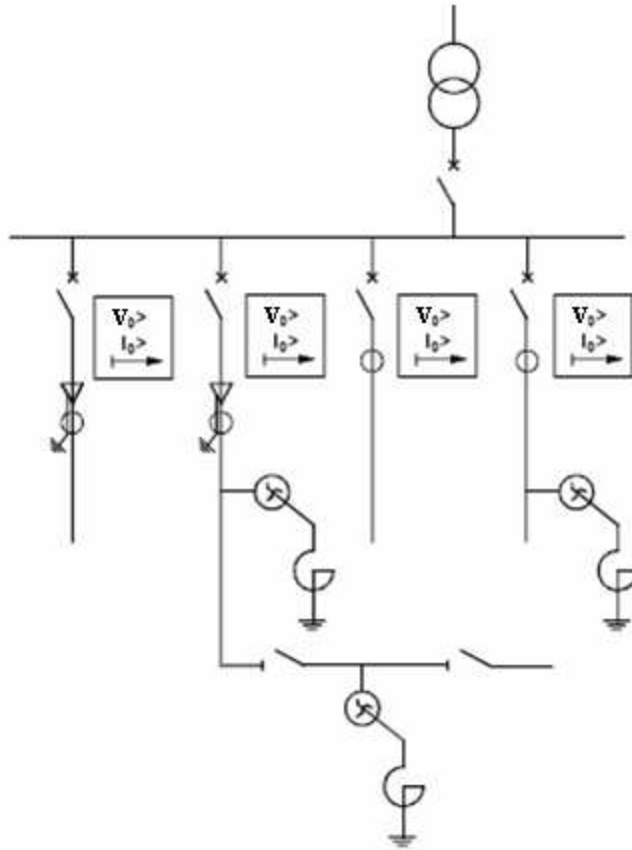


**Figure 12.** Decentralized compensation at MV network. (Pouttu 2007a: 31)

### 3. FUNDAMENTALS OF NETWORKS FAULT SITUATIONS

#### 3.1. Faults concept

There are two types of faults in the network. First, we have symmetrical faults. These faults are easy to calculate because network can be translated to a simple single-phase equivalent circuit. Symmetrical fault is a three-phase short circuit. Secondly, we have asymmetrical faults. These faults are more common than symmetrical faults. The most common fault causing asymmetry is an earth fault. When faults are asymmetrical, network can no longer be transformed to a single-phase equivalent circuit and the whole network has to be treated as a three-phase circuit in its original form. (Kothari & Nagrath 1994: 420)

##### 3.1.1. Symmetrical faults

Symmetrical fault is a very rare situation. As mentioned before, a three-phase short circuit is a symmetrical fault. Although this type of fault is very rare, it has to be taken care of, because it's the most severe accident the power delivery system will face. One of the common three-phase short circuits is generator fault. The fatality is caused by very big fault current. Big current is produced, because limiting inductances are very small. The fault starts from the sub transient current, which leads to the steady-state fault current values. Fault detection and clearing has to be very fast in order to limit disturbances to the power system.

##### 3.1.2. Asymmetrical faults

More often occurring fault is asymmetrical fault. When fault is asymmetrical, fault currents and voltages are not equal at different phases. There are two main types of asymmetrical faults: shunt type and series type faults. Shunt type fault is a connection between two network elements. Series type means broken connection at the conductor. The most common asymmetrical fault is an earth fault. Asymmetrical fault indicates itself easily and from the phase values it is easy to acquire what type of asymmetrical

fault it is. The studies of the network's asymmetrical faults are important because of the network protection. Studies are usually carried out by the method of the symmetrical components. (Kothari etc. 1994: 449)

### 3.2. Basic theory and data of earth fault

Earth fault is a situation where non-earthed, live part of the network is connected to the earth through relatively low impedance. It can be a permanent fault, which requires the personnel to rectify the fault situation, or it can be a transient fault, which can be managed via automatically controlled protection system. Critical issue at earth fault is the magnitude of fault resistance. If magnitude is relatively high, electricity supply can be continued even if the fault is permanent.

Four basic types can classify earth fault types. These types are shown in the figure 13. The simplest type is single-phase to earth fault as shown in point 1. This is most commonly caused by wire drop. Second alternative is a 2-phase earth short circuit as shown in point 2. In this fault type, two different phases are short circuited together with the earth. Third alternative is a double earth fault, where two different phases are simultaneously connected to the earth at the different locations. This alternative is shown in point 3. Fourth fault type is cut wire, where load side is connected to the earth as shown in point 4.

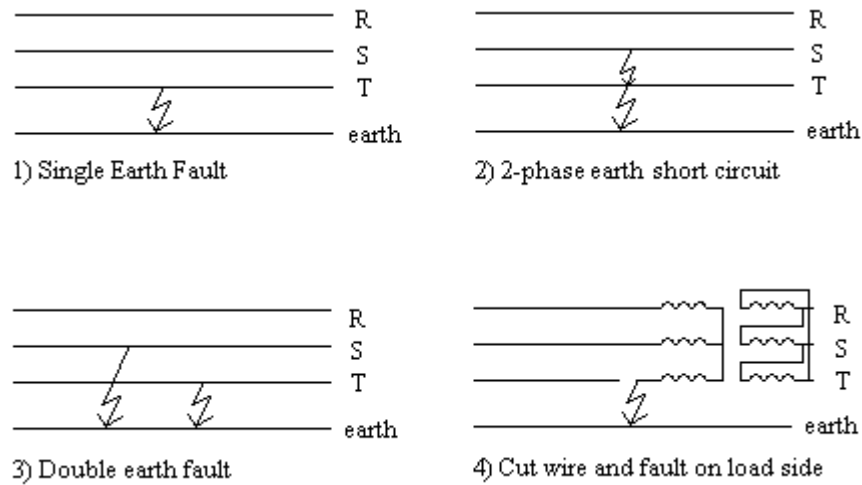


**Figure 13.** Illustration of different types of earth faults.

Most common reasons to earth faults are, for example, arcs during lighting; trees, which have fallen to conductors; and animals, which are moving near live wires. It is usual that during the earth fault there are also some other faults.

Harmful effects of the earth fault can be measured by two alternative ways. First of all, you have to measure whether the fault is fatal to human beings. Second, you have to measure how harmful the fault is to the property.

It is estimated that 80 – 90 % of the faults in the MV network are earth faults. In some cases, earth faults may lead up to more complex situations like 2-phase earth faults. Although the number of earth faults is large, they are usually temporary. Today's relay technology has also improved the situation. When modern protection relays have artificial intelligence, they normally are able to reclose network after the arc is cleared. (Pouttu 2007a: 24 - 26)

### 3.3. Basic measurements at fault situation

Basic measurements during the faults are carried out with voltage or current transformers. Also combination is possible. Transformers are used, because the values are too high to be measured directly. Both magnitude and angle values are needed. Measured

values are normally compared to known healthy state values. If any changes occur, needed operations are carried out.

An earth fault situation at the compensated network is always challenging for feeder protection. When determining values for protection, many variables have to be known. Length of cable and type of cable are some issues to be mentioned. In the earth fault calculations the network is simplified to a partial network, which contains only crucial components. This makes calculations and logical deduction much easier.

### 3.4. Earth fault in the compensated network

When earth fault occurs, fault resistance connects to series with parallel connection of compensation equipment and earth capacitance. Main benefit of compensation is that most of the earth faults clear by themselves. Other benefit is that in an arcing situation restriking is unlikely, because of slow increase of the arcing voltage. Some benefits can also be gained, when the use of the network can be continued despite permanent earth fault existing in rural conditions. Figure 14 shows the equivalent circuit of earth fault in a compensated network. (Hakola etc. 1996: 18)

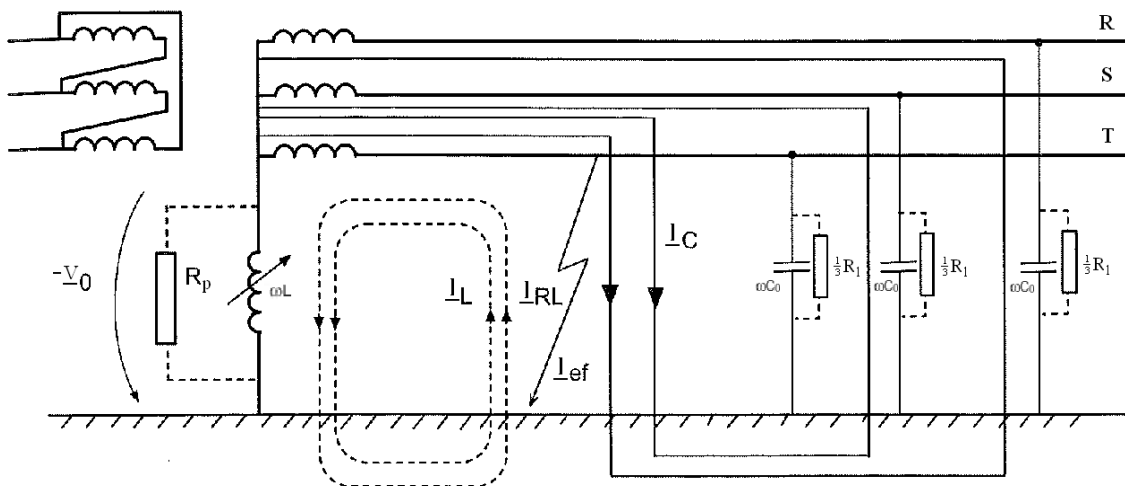


**Figure 14.** Basic illustration of earth fault of compensated network. (Hakola etc. 1996:

In the diagram there are four different currents.  $I_{ef}$  is earth fault current,  $I_{R1}$  is leak current through line or cable insulations,  $I_L$  is current through Petersen coil and  $I_C$  is current through earth capacitance of network. Two resistances are introduced.  $R_1$  is leakage resistance and  $R_p$  is Petersen coils parallel resistance.  $\omega L$  is Petersen coil and  $\omega C_0$  is earth capacitance of single-phase. In a fault situation it is possible to reduce the whole network to one Thevenin connection shown in the figure 15.

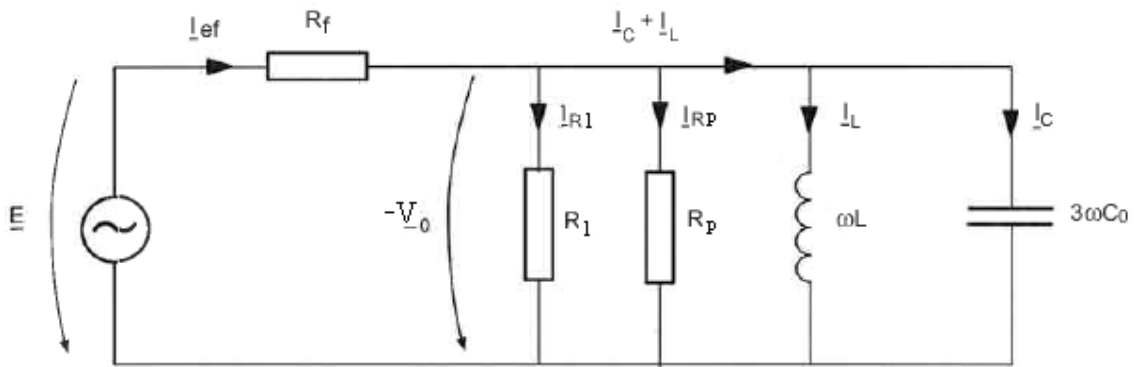


**Figure 15.** Single-phase equivalent circuit of compensated networks earth fault. (Hakola etc. 1996: 17)

At the previous circuit diagram  $E$  is line-to-line voltage. In the diagram there are five different currents.  $I_{ef}$  is earth fault current,  $I_{R1}$  is leak current through line or cable insulations,  $I_{Rp}$  is current through Petersen coils parallel resistance,  $I_L$  is current through Petersen coil and  $I_C$  is current through earth capacitance of network. Three resistances are introduced.  $R_f$  is fault resistance,  $R_1$  is leakage resistance and  $R_p$  is Petersen coils parallel resistance.  $\omega L$  is Petersen coil and  $3\omega C_0$  is earth capacitance of network. Fault current and neutral point voltage can be calculated with simple equations. (ABB 2000) Fault current is

$$I_{ef} = \frac{E \sqrt{1 + R_p^2 \left(3\omega C_0 - \frac{1}{\omega L}\right)^2}}{\sqrt{(R_f + R_p)^2 + R_f^2 R_p^2 \left(3\omega C_0 - \frac{1}{\omega L}\right)^2}} \quad (3)$$



and neutral point voltage is

$$U_s = \frac{I_{ef}}{\sqrt{\left(\frac{1}{R_p}\right)^2 + \left(3\omega C_0 - \frac{1}{\omega L}\right)^2}} . \quad (4)$$

When compensation is near 100 %, both fault current and neutral point voltage can be calculated with much more simpler equations. Fault current is then

$$I_{ef} = \frac{E}{R_p + R_f} \quad (5)$$

and neutral point voltage is then

$$U_s = \frac{ER_p}{R_p + R_f} . \quad (6)$$

### 3.5. Equation to determine size of compensation coil

All the calculations rely on circuit diagram presented on the page 32 in the figure 15. Conductor's leak resistance is not taken into account. First admittance  $\underline{Y}$  of parallel connection of Petersen coils inductance, earth capacitance and grounding resistances is calculate by utilizing equation

$$\underline{Y} = \frac{1}{R_p} + \frac{1}{jX_L} + jX_c , \quad (7)$$

where  $X_L$  is reactance of Petersen coil and  $X_c$  is networks earth capacitance. Then fault resistance is added to equation

$$\underline{Z} = R_f + \frac{1}{\underline{Y}} , \quad (8)$$

If total compensation level is wanted to be reached, imaginary part of  $\underline{Z}$  is set to be zero. The capacitance of the network is constant so inductance is the value to be determined as shown in the equation

$$X_L = \frac{1}{X_C}. \quad (9)$$

Different compensation levels can be acquired by setting desired compensation degree  $k$  to the relation equation

$$X_L = \frac{1}{kX_C}. \quad (10)$$

If for example 80 % compensation degree is tried to be reached,  $k$  is set to 0,8.

### 3.6. Introduction to the symmetrical components

It's a common fact that calculations concerning three-phase network are hard, even when carried out by computer. Normally, in this situation a calculation method called symmetrical components is introduced. When symmetrical components are used, network's current and voltage values are resolved to three vector components called positive, negative and zero sequence components. (Kothari etc. 1994: 421)

The transformation is carried out from phase voltages  $\underline{U}_R$ ,  $\underline{U}_S$  and  $\underline{U}_T$ . At the transformation phase shifting operator  $a$  is needed. Its numerical form is  $1 \angle 120^\circ$ . First system to introduce is zero sequence voltages. Every zero sequence voltages have same phase angle and magnitude  $\underline{U}_{R0} = \underline{U}_{S0} = \underline{U}_{T0} = \underline{U}_0$ . Second and third systems are known as positive and negative sequence systems. Positive voltage sequences are  $\underline{U}_{R+} = \underline{U}_+$ ,  $\underline{U}_{S+} = a^2 \underline{U}_+$  and  $\underline{U}_{T+} = a \underline{U}_+$ . Negative voltage sequences are  $\underline{U}_{R-} = \underline{U}_-$ ,  $\underline{U}_{S-} = a \underline{U}_-$  and  $\underline{U}_{T-} = a^2 \underline{U}_-$ . Each voltage has 120 or -120 degrees difference to other voltages at the same sequence. The original voltages are sum of each sequence voltage vectors. For example  $\underline{U}_R = \underline{U}_{R0} + \underline{U}_{R-} + \underline{U}_{R+}$  (Nagrath etc. 1994: 421 - 422)

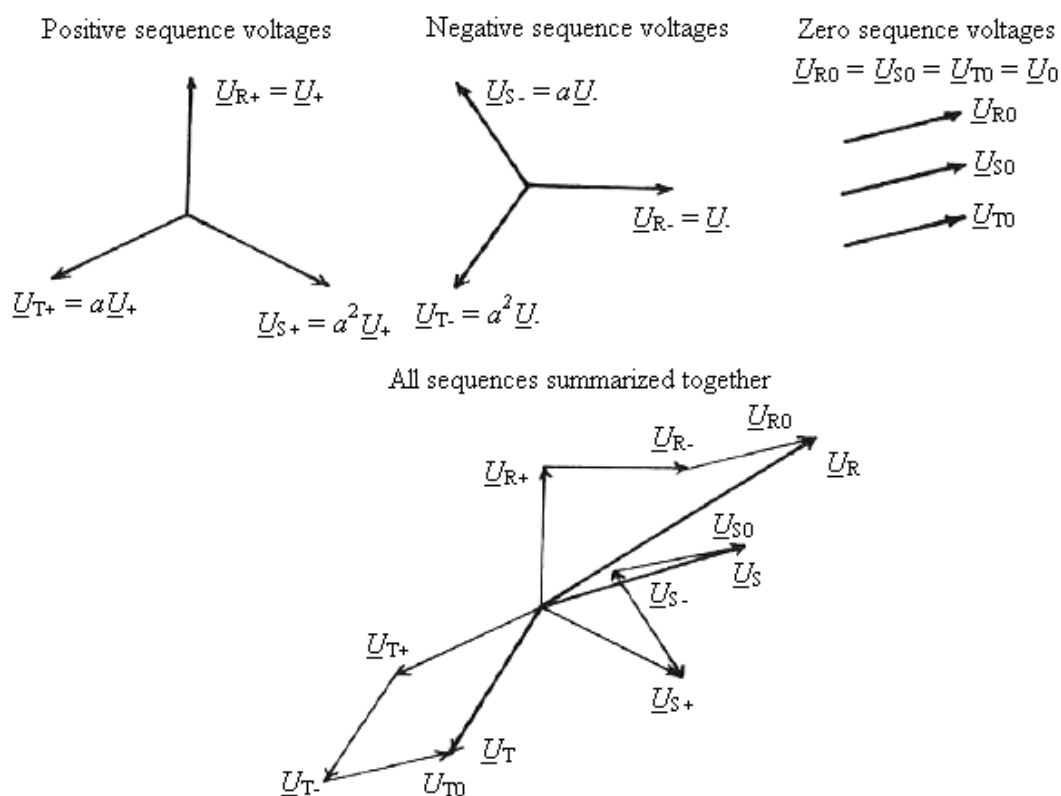


**Figure 16.** Basic example of relation between phase values and symmetrical values.

### *Symmetrical components transformation matrixes*

Transformations from phase values to symmetrical values are carried out via three equations formed to a matrix. The main equation for this matrix is

$$\underline{V}_p = A \underline{V}_s, \quad (11)$$

where  $\underline{V}_p$  is phase voltage vector,  $A$  is symmetrical component transformation matrix and  $\underline{V}_s$  is symmetrical voltage vector. The transformation matrix  $A$  is

$$[A] = \begin{bmatrix} 1 & 1 & 1 \\ 1 & a^2 & a \\ 1 & a & a^2 \end{bmatrix}. \quad (12)$$

When the equation 11 is used, the matrix equation

$$\begin{bmatrix} \underline{U}_R \\ \underline{U}_S \\ \underline{U}_T \end{bmatrix} = \begin{bmatrix} 1 & 1 & 1 \\ 1 & a^2 & a \\ 1 & a & a^2 \end{bmatrix} \begin{bmatrix} \underline{U}_0 \\ \underline{U}_+ \\ \underline{U}_- \end{bmatrix} \quad (13)$$

has got. At matrix voltages  $\underline{U}_R$ ,  $\underline{U}_S$  and  $\underline{U}_T$  are phase voltages and  $\underline{U}_0$ ,  $\underline{U}_+$  and  $\underline{U}_-$  are zero sequence, positive sequence and negative sequence voltages. For currents the same transformation is applied to matrix

$$\begin{bmatrix} \underline{I}_R \\ \underline{I}_S \\ \underline{I}_T \end{bmatrix} = \begin{bmatrix} 1 & 1 & 1 \\ 1 & a^2 & a \\ 1 & a & a^2 \end{bmatrix} \begin{bmatrix} \underline{I}_0 \\ \underline{I}_+ \\ \underline{I}_- \end{bmatrix}, \quad (14)$$

where currents  $\underline{I}_R$ ,  $\underline{I}_S$  and  $\underline{I}_T$  are phase currents and  $\underline{I}_0$ ,  $\underline{I}_+$  and  $\underline{I}_-$  are zero sequence, positive sequence and negative sequence current.

Reverse operation is also needed. The transformation matrix for this operation can be derived from matrix  $A$ , which is presented on the page 35 in the equation 12. The transformation matrix for reverse operation is

$$A^{-1} = \frac{\text{adj}(A)}{\det(A)} = \frac{1}{3} * \begin{vmatrix} 1 & 1 & 1 \\ 1 & a & a^2 \\ 1 & a^2 & a \end{vmatrix} \quad (15)$$

and the equation for converting symmetrical voltages to phase voltages is

$$\begin{bmatrix} \underline{U}_0 \\ \underline{U}_+ \\ \underline{U}_- \end{bmatrix} = \frac{1}{3} * \begin{bmatrix} 1 & 1 & 1 \\ 1 & a & a^2 \\ 1 & a^2 & a \end{bmatrix} \begin{bmatrix} \underline{U}_R \\ \underline{U}_S \\ \underline{U}_T \end{bmatrix} \quad (16)$$

and the equation for converting symmetrical currents to phase currents is

$$\begin{bmatrix} \underline{I}_0 \\ \underline{I}_+ \\ \underline{I}_- \end{bmatrix} = \frac{1}{3} * \begin{bmatrix} 1 & 1 & 1 \\ 1 & a & a^2 \\ 1 & a^2 & a \end{bmatrix} \begin{bmatrix} \underline{I}_R \\ \underline{I}_S \\ \underline{I}_T \end{bmatrix}. \quad (17)$$

At the earth fault protection, normally only zero components of symmetrical components are used. (Kauhaniemi 2007)

## 4. EARTH FAULT PROTECTION

### 4.1. Microprocessor-based relay

The protection of distribution network is a complex issue. Key solution for this challenging procedure today is a microprocessor-based relay. It can protect sensible parts of the network with good accuracy. This is possible by relays ability to monitor massive amounts of network values. Before, it was common that one relay measured only one value. Revolution happened when mechanical relays where replaced by microprocessor-based units. The basic principle is to convert analog data from the network to digital form. Illustration of operation principle of a numerical relay is shown in the figure 17.

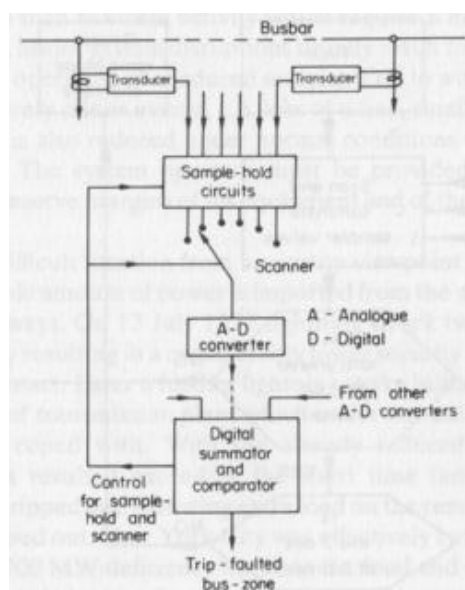


**Figure 17.** Basic diagram of a numerical relay. (Weedy 1987: 511)

The values, which can be processed through modern relay, can include for example: current, voltage, frequency and power. From these values it is possible to measure the differential between measured values, asymmetry between different phase angles, and even determine the fault location. Normal setting values include, for example, tripping delays. The basic diagram of normal protection relay algorithm is shown in the figure 18.

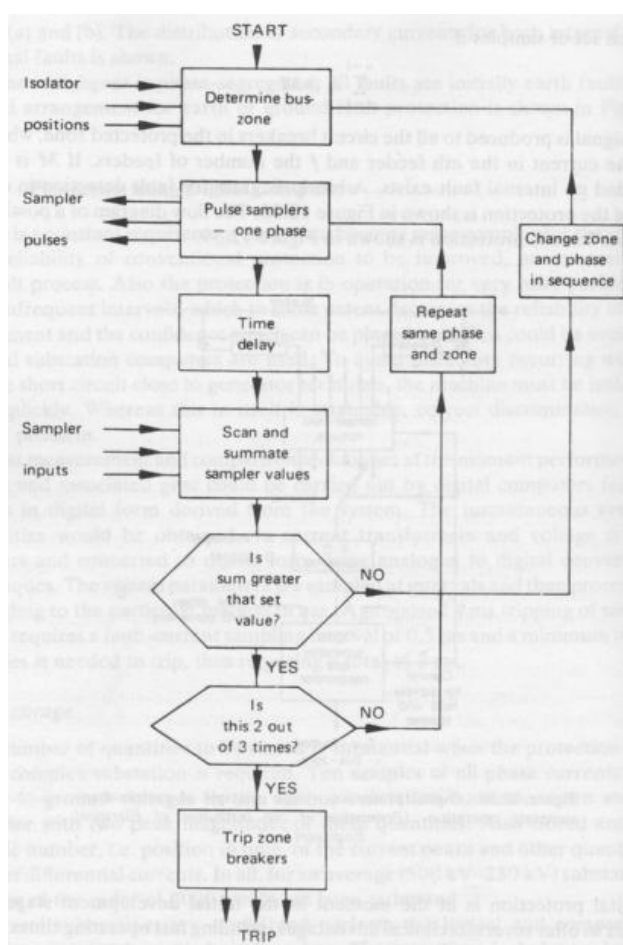


**Figure 18.** Basic diagram of a typical protection relay program. (Weedy 1987: 512)

Although the accuracy is the best characteristic of a microprocessor-based relay, nearly as beneficial feature is data recorder. It makes possible to view fault situations after the fault, and monitor what really happened.

#### 4.2. Operational characteristics

Protection methods, which are in use in this thesis, have each their unique operational characteristic. Examples of typical operation characteristics are shown in figures 19, 20 and 21. They are applied to directional earth fault protection in compensated networks, which is the main topic of this thesis. Operation characteristics define the borders be-

tween operational and non-operational areas. Usually the marked area is the operational area, but in case of admittance characteristic, it defines the non-operational area.

In case of residual current based earth fault protection functions, the operation characteristic is drawn such that the vertical axis is taken as reference and it represents the phase angle of the polarizing quantity. Typically this quantity is the residual voltage  $\underline{U}_0$ . Normally the characteristic is drawn so that the  $-\underline{U}_0$  vector is taken as reference.

The left hand side of the operation characteristic indicates capacitive current and the right hand side inductive current. When the measured value moves from non-operational area to operational area, desired operations would be carried out. Example of this operational characteristic is shown in the figure 19.

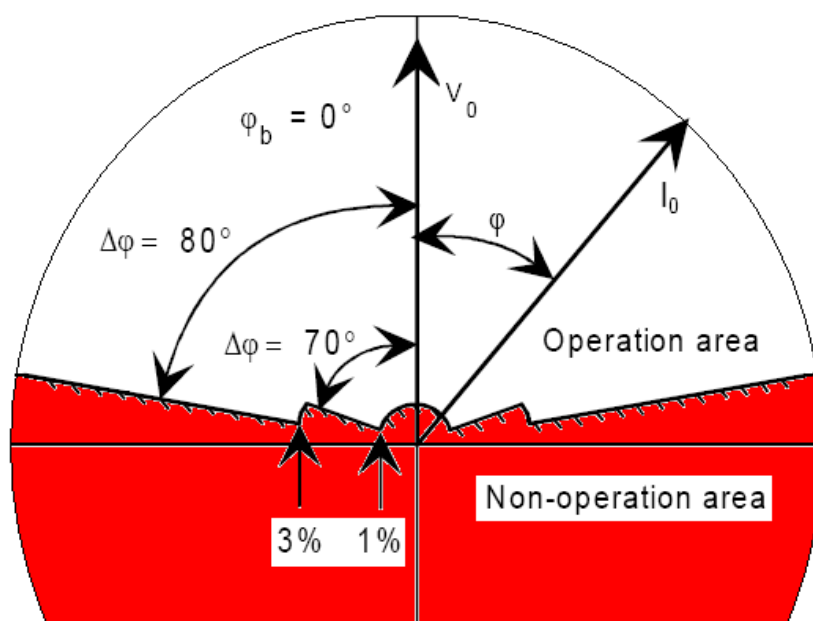


**Figure 19.** Operational characteristics with vectors  $\underline{I}_0$  and  $\underline{U}_0$ . Operational area is colored with white and non-operational with red. (ABB 2005: 11)

Another common way to show operational characteristics is to use  $\varphi$  versus  $\underline{I}_0$  or  $I_0 \cos(\varphi)$  characteristic. In the horizontal axis there is phase angle  $\varphi$  and in the vertical axis there is amplitude of zero sequence current  $\underline{I}_0$  or  $I_0 \cos(\varphi)$ . When measured value



moves inside the operational area, desired operations would be carried out. Example of this operational characteristic is shown in the figure 20.

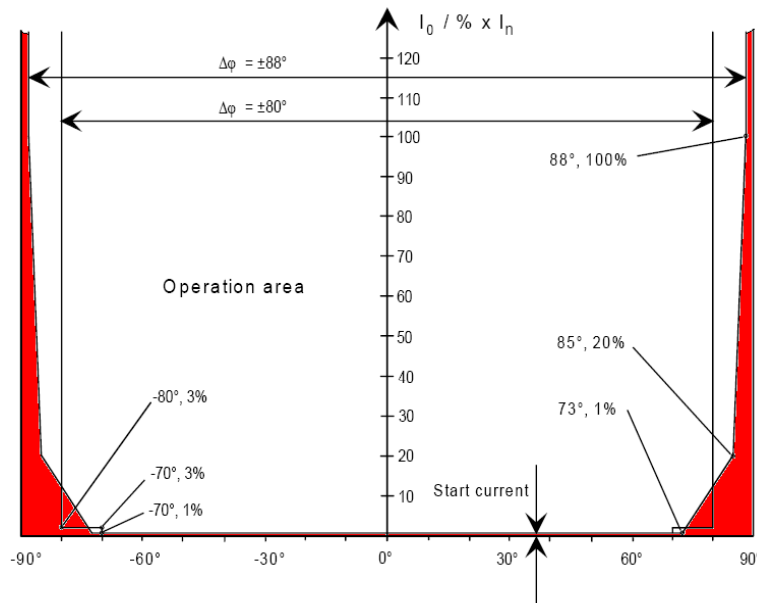


**Figure 20.**  $I_0$  versus  $\varphi$  operational characteristics. Operational area is colored with white and non-operational area is colored with red. (ABB 2005: 11)

Admittance based operational characteristics are also used. Limits can be set for either total magnitude of admittance or real or imaginary part of the admittance. For these parts terms susceptance and conductance are often used. Combinations of previously mentioned limits can be also used. Typical admittance operational characteristics are shown in the figure 21. It should be noted that operation is achieved, when operation point moves outside the characteristics.

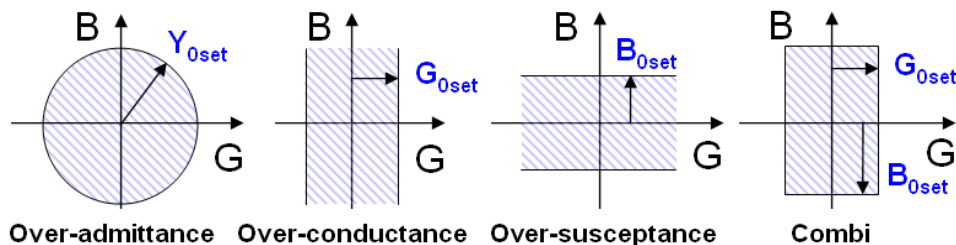


**Figure 21.** Examples of admittance operational characteristics. (Altonen & Wahlroos 2009)

### 4.3. Elements of the protection system

The network is built from different elements which all have different tasks. Those elements can be divided to power carrying, measuring and protecting elements. Power carrying elements are transmission lines, transformers, generators and loads. Measuring elements are instrument transformers and sensors. These sensors provide information to the protection elements. Protection relays and switches are protection elements. These elements form the main network, which is measured and studied in this thesis.

At case of this thesis, measurements for the protection elements are carried out at the beginning of the studied feeder. The needed values vary depending on the protection methods, but the overall currents and voltages from each phase are needed. For earth fault protection zero sequence current  $I_0$  and  $U_0$  zero sequence voltage measurements are enough. However, also phase angle between  $I_0$  and  $U_0$  is relevant information. When angle information is used, protection method is called directional protection. This thesis concentrates on four different protection methods which all are directional. (Pouttu 2007a: 54)

#### 4.3.1. Instrument transformers and sensors

Instrument transformers are special voltage and current transformers, which are built to measure values from the electrical network. When using instrument transformers, it is possible to protect sensitive protection relays of dangers of primary system. These dangers include, for example, network overvoltages. Galvanical separation of measurement circuit from the primary system is also benefit. An instrument transformer also allows setting up measuring equipment far away from the measuring point itself. Standardization of monitored values is also an important issue. When measurements are carried out, current transformers secondary windings load resistance should be held near zero and voltage transformer's secondary windings load resistance should be held near infinite. All instrument transformers are graded by their transformation accuracy. Normally there are two different protection classes, which are 5P, which allows  $\pm 1\%$  current error, and 10P, which allows  $\pm 3\%$  current error. Current error can be calculated with a simple equation

$$F_i = \frac{K_n I_s - I_p}{I_p} 100 \% , \quad (18)$$

where  $F_i$  is current error,  $K_n$  is transformation ratio,  $I_s$  is rms value of secondary windings current and  $I_p$  is rms value of primary windings current. Basically this means that the current transformer should be selected to work properly with the highest magnitude of fault current.

The voltage transformer provides voltage signal to the meters and protection relays. Usually these transformers have only one iron core. Open delta connection is introduced to serve earth fault protection procedures. One point of voltage transformer's secondary winding always has to be always grounded to avoid harmful over and touch voltages. The structure of voltage transformer is today always a group of three single-phase voltage transformers.

Current transformers are more complicated devices than voltage transformers. The changes in the measured current are always much larger than changes in measured voltage, which makes the construction more complex. When voltage transformer typically has only one core, current transformer always has more. Often there are separate windings for protection and measurement purposes at the secondary side of the transformer. Current transformers are manufactured to work properly when electricity has frequency of 50 Hz and measured values are sinusoidal. Commonly used transformation ratios are 150:5 A and 100:1 A. In the past, widely used ratio was 200:1 A. Transformers are always fitted to suit for the requirements of the protection relays needs. Current transformer's secondary winding has to always be closed. If the circuit is opened, voltage between terminals will increase to harmful levels. (ABB 1999: 190, 239; Hakola etc. 1996: 73 – 74; Mörsky 1993: 85 - 87, 101 - 105)

The most common way to deal with current measurements is to use current transformer. Saturation and too big current range are normal causes of problems, when working with current transformers. Saturation can be avoided by choosing as correct as possible transformation ratio, but large current range is a bigger problem. For example, at the compensated network, current transformers handle currents, which are much lower than

nominal current. When working far away from the nominal current, especially on lower side, error at transformation increases to unwanted levels. This is usually avoided by using single-phase transformers, which are produced in the same manufacturing lot. By doing so differences in manufacturing is tried to be minimized. To minimize calculation errors, summarization of currents has to be carried out near current transformers. (Mörsky 1993: 130 - 133)

When choosing current transformer, the amount of DC component produced by the network, should be also taken into account. DC causes saturation. The only way to get rid of DC current problem is to introduce different types of sensors or simply try to make the network produce less DC current.

In some cases, and probably more in the future, there are some alternatives for current transformer. For example, Rogowski coil can be introduced to replace the traditional current transformer. During the past, Rogowski coils use has been limited; because the coils output is proportional to the time derivate and it has to be integrated. The revolution of microprocessors in past decades has made this drawback into a minor problem, and today, this solution has become really interesting. The best benefit of Rogowski coil is that, it has air core, and thus it has no non-linear effects like saturation. Current sensors, which use principle of Rogowski coil, are also usually cheaper than those, which have been made in traditional way. It is also good option for temporary measurement purposes, because it can be installed to live network. (Nikander 2002: 30 - 31)

#### 4.3.2. Earth fault current compensation equipment

Fault current in unearthed network is always reactive because of overhead line's and cable's earth capacitance. According to the law of determining capacitance of capacitor, earth capacitance is always bigger when cable network is introduced. (Kervinen & Smolander 2000: 118)

Current compensation equipment is a device, which is connected to the neutral point of HV to MV transformer stations MV side. It can also be called Petersen coil, by the name of its inventor. The basic principle is to add inductance in parallel with network's

earth capacitance. Inductance can be fixed, controlled by certain steps, or continuously controllable by local or remote control. Normally 80 – 120 % compensation levels are used, but due the specifications of protection procedure exact 100 % compensation level cannot be applied.

A resistor can be also added into parallel connection with the compensation coil, to increase resistive fault current. This is carried out to ensure proper functioning of the directional protection. If resistive current is absent, directional protection won't work.

There are three possible ways to add a resistor. First, it can be continuously connected. Second, it can be connected after a small delay when fault occurs. Third way to connect the resistor is to disconnect it when fault occurs and connect it back, if the fault is not cleared after a certain period of time. During the recent research made in Finland's 20 kV MV network, it is suggested that the parallel resistance of the Petersen coil should be permanently switched on to achieve best operation conditions for admittance protection. The most critical issue this is, when the algorithm utilizes pre-fault values. On the other hand, certain fault location algorithms require the connection of parallel resistance during the fault in order to enable fault distance calculation. (Altonen etc. 2009)

When the compensation equipment is part of the network, it also needs protection. Normally it is carried out with, for example, a winding temperature detector or a Buchholz relay. These protection and compensation equipment also need power. This power is normally taken from the compensation coil by using it as a transformer by adding a "secondary winding" along the coil. In the design of compensation equipment, this has to be taken into account. (Hakola etc. 1996: 64 - 70)

#### 4.4. Protection methods

Protection methods are always based on one or more values derived from the network. The final value can be reached via simple calculations. However, all methods used in this thesis have  $\underline{U}_0$  as a trigger. Fault is detected only after  $\underline{U}_0$  has risen above its setting value.

When traditional protection methods are designed, due to limited calculation power of protection relays, they are designed to be simple. The simpler the calculation algorithm is, the faster it is. The less clock cycles is needed, the more reliable the protection method usually is. During today's era of powerful microprocessors this is a minor problem. In this thesis, main attention is paid to protection methods, which are proven to be good for normal earth fault protection procedures. Novel protection method called admittance protection method is also used. All used protection methods are described in detail in following sections.

#### 4.4.1. Base Angle criterion

Base angle criterion measures zero sequence voltage  $\underline{U}_0$  and zero sequence current  $\underline{I}_0$ . Vectors  $\underline{U}_0$  and  $\underline{I}_0$  have their maximum magnitude setting values. If these values are exceeded desired operation will be carried out. The angle  $\varphi$  between zero sequence current and voltage is also derived. Normally the operation sector is  $\pm 80$  degrees or 160 degrees. So, if the middle point of the operation sector is -90 degrees, the area where angle  $\varphi$  can travel is from -170 degrees to -10 degrees. In the isolated neutral system, the middle point of the operation sector is usually set to -90 degrees and in compensated network to 0 degrees. Setting values for zero sequence current and voltage depend on e.g. parameters of network and instrument transformers. It is essential to remember that in this protection procedure, both magnitude and angle values are used. The magnitude or the angle cannot alone cause protection relay tripping. Normal operation characteristics are shown on the page 39 in the figure 19 (Pouttu 2007a: 57)

#### 4.4.2. $I_0 \cos(\varphi)$ protection method

$I_0 \cos(\varphi)$  express network's resistive current. This method is widely used in compensated networks. In the compensated network, which is driven with 100 % compensation degree, the fault current consists mainly of resistive current. The amount of reactive current depends on compensation degree. When the amount of resistive current increases, the phase angle moves to the direction of resistive current. The direction where the angle goes depends on whether the network is driven under- or over-compensated. When

the current has been increased enough, the angle moves to operational area and desired operations are carried out. (Pouttu 2007a: 57 - 60)

#### 4.4.3. Wattmetric protection method

A basic principle of Wattmetric is to measure zero sequence value's active power. It's  $I_0 \cos(\varphi)$  value multiplied with magnitude of zero sequence voltage  $\underline{U}_0$ . The sign (plus or minus) tells if the fault is at a protected feeder or not. Although Wattmetric is an old protection method, it is still a powerful way to detect low resistance earth faults. The negative aspect of this protection method is that it cannot detect high resistance earth faults, if the parallel resistor of the Petersen coil is not used. The limit goes somewhere near 3 k $\Omega$  – it depends a lot on the protection adjustments. For example, a tree fallen over the lines usually cannot be detected by the Wattmetric method without use of the Petersen coils parallel resistance (Pouttu 2007a: 62)

As mentioned before, Wattmetric protection is more effective, if an additional parallel grounding resistance is introduced. It has a direct effect on the ability to detect high resistance earth faults. By doing so, the limit to detect earth faults can be stretched to 5 k $\Omega$ . General rule is that, when using Wattmetric, network should be driven little over-compensated. (Pouttu 2007a: 62)

When Wattmetric method is used, measurement accuracy is really important. When the measured values are small, even a small error causes big difference in the final values. To make values more readable, usually applicable resistance is connected in parallel with the compensation coil. Proper fitting is necessary, because if the resistance is too small, the neutral point voltages magnitude  $U_0$  shrinks too much, and if it's too big, it renders useless. Parallel resistance is usually automatically controlled by pre-programmed logic. At the overall, when Wattmetric is supported by other protection methods, e.g. residual overvoltage protection, it is a decent method to take care of earth fault protection. Even then the setup of Wattmetric has to be configured carefully. (Pouttu 2007a: 62 - 64)

#### 4.4.4. Neutral Admittance protection method

Neutral admittance method is based on zero sequence voltage  $\underline{U}_0$  and zero sequence current  $\underline{I}_0$ . By the law of ohm, admittance is reached by dividing current vector  $I$  by voltage vector  $U$ . Result of this division is also a vector and normally this vector is placed in admittance plane where horizontal axis shows conductance and vertical axis shows susceptance. In recent tests, it has been shown that this method is a good earth fault protection method in, for example, unearthed and compensated networks. Strengths of neutral admittance protection method are, for example, immunity against different sizes of fault resistance, and easy setting principle. When using this protection method, it is suggested that parallel resistance of Petersen coil is permanently connected. Even though this protection method is rather new, it is already widely in use in Poland. (Altonen etc. 2009)



## 5. DISTRIBUTION NETWORK TO BE STUDIED

In this thesis, two different models of distribution network are studied. The only difference between these models is the number of the feeders of the background network. The network is modelled at the PSCAD power system simulator and the data from the simulations is filtered with Matlab® scripts. A basic type of studied network is shown in the figure 22. At this figure the background network consist of 5 feeders.

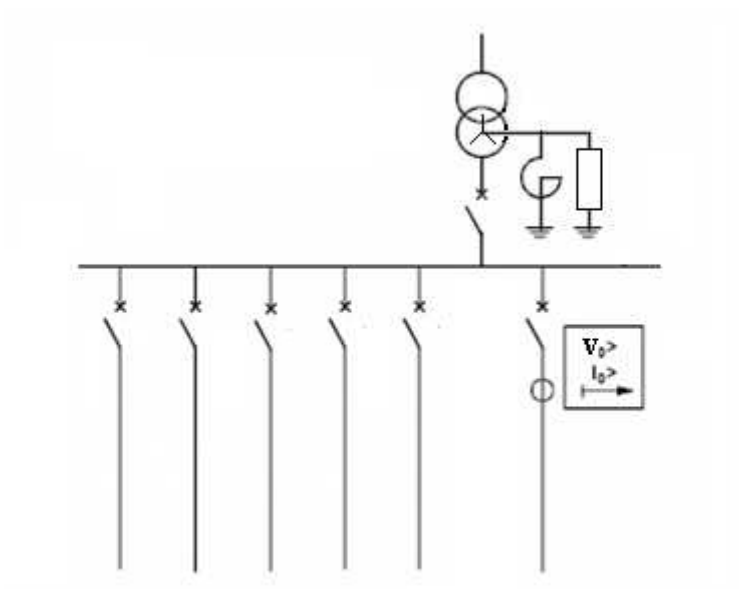


**Figure 22.** Basic illustration of studied network with five background network feeders.

### 5.1. Network parameters

In the MV network model, there are lots of parameters to be chosen. During this thesis, only some key parameters are varied, while others are kept constant during all the simulation. Parameters that are held constant in this thesis are: the voltage of network, number of studied feeders and the state of switch controlling the Petersen coil's parallel resistance. Varied parameters are: length of the studied feeder, location of the fault, and compensation degree. Some special simulations are carried out by changing value of fault resistance, value of Petersen coil's parallel resistance and size of background net-

work. During the simulation, where size of background network is valued, it is carried out by either changing value of reactive fault current or number of background network feeders.

#### *Parameters used at this thesis*

Because of the large number of variable parameters, the number of simulations will easily increase to a too high level. Selection of which parameters are varied, and the range and steps of the variations, should be made carefully. Parameters involved are presented in the following, starting from the ones that are kept constant.

The voltage level has very well known effects to the network, and it was chosen to keep it at a constant value of 10 kV. The number of studied feeders was also easy to set to only one feeder, because the same fault values occur in every equal feeder. The hardest-to-choose constant parameter was the switching type of Petersen coil's parallel resistance. There are three possibilities, which are taken from Active Current Forcing, ACF, scheme. First the resistor can be switched on all the time. Secondly it can be switched on after some delay, when the fault occurs. Thirdly and finally the resistor is switched on and when the fault occurs, it is temporarily switched off. The final choice for that parameter was to set it on all the time. In the simulations, there are no problems with this issue, but in real life, current through this resistance cannot be very large. This has to be taken into account, because a resistance always produces heat and this heat production is increased to square when the current increases. In the main part of the simulations the Petersen coil's parallel resistance current value is held at 10 A, fault resistance  $R_f$  is zero and value of the background network's fault current is 150 A (Altonen etc. 2009)

The varying parameters included length of the feeder, compensation degree, and the location of the fault. The magnitudes were chosen by doubling 7 km feeder length, until a big enough factor was reached. This feeder length was 56 km and it gave four sensible variations: 7, 14, 28 and 56 km.

Level of compensation includes all compensation types. 80 % represents under-compensation, 100 % total compensation and 120 % over-compensation. When 4 length variables and 3 compensation variables are multiplied, it totals to 12 simulations to make, so the number of possible fault locations is limited to three to limit the number of simulation runs to sensible level. Fault locations where fault occurs at the beginning of the studied feeder, at the middle of the feeder and at the end of the feeder are used. Corresponding numerical forms of these locations are 0, 0.5 and 1. Parameters of all basic simulation cases are shown in table 1. At the table 1, “length” is length of studied feeder, “comp” is compensation degree and “location” is fault location.

**Table 1.** Parameters used in the basic simulation cases.

length	comp	location	length	comp	location	length	comp	location
7 km	80 %	0	7 km	80 %	0.5	7 km	80 %	1
14 km	80 %	0	14 km	80 %	0.5	14 km	80 %	1
28 km	80 %	0	28 km	80 %	0.5	28 km	80 %	1
56 km	80 %	0	56 km	80 %	0.5	56 km	80 %	1
7 km	100 %	0	7 km	100 %	0.5	7 km	100 %	1
14 km	100 %	0	14 km	100 %	0.5	14 km	100 %	1
28 km	100 %	0	28 km	100 %	0.5	28 km	100 %	1
56 km	100 %	0	56 km	100 %	0.5	56 km	100 %	1
7 km	120 %	0	7 km	120 %	0.5	7 km	120 %	1
14 km	120 %	0	14 km	120 %	0.5	14 km	120 %	1
28 km	120 %	0	28 km	120 %	0.5	28 km	120 %	1
56 km	120 %	0	56 km	120 %	0.5	56 km	120 %	1

To get more value for the simulations, some special cases are also studied. All these simulations are made in 100 % compensated network, and the fault is located at the middle of the feeder unless otherwise stated. Feeder lengths of 14 and 28 km are used. In the first special case, fault resistance is increased from 0  $\Omega$  to 3 k $\Omega$ . In the second special case, value of the fault current provided by the background network is doubled from 150 A to 300 A. Third special simulation has 10 background network feeders instead of 5. Fourth and the last special simulation is run with larger Petersen coil parallel resistance value of 30 A instead of normal 10 A. At this simulation, 80 % and 100 % compensation levels are used. An earth fault in the background network is also studied, but it is simulated only with feeder lengths of 14 and 28 km and compensation levels

80 % and 100 %. Parameters of all special simulation cases are shown in the following table. At the table 2  $R_f$  is the fault resistance, “nbgw” is the number of background network feeders,  $I_{bgw}$  is the magnitude fault current produced by background network and  $I_{Rp}$  is the current of the Petersen coils parallel resistance.

**Table 2.** Simulation parameters used in special simulation cases.

length	comp	location	$R_f$	nbgw	$I_{bgw}$	$I_{Rp}$
14 km	100 %	bgw	0	5 pi	150 A	10 A
28 km	100 %	bgw	0	5 pi	150 A	10 A
14 km	80 %	bgw	0	5 pi	150 A	10 A
28 km	80 %	bgw	0	5 pi	150 A	10 A
14 km	100 %	0.5	3 k $\Omega$	5 pi	150 A	10 A
28 km	100 %	0.5	3 k $\Omega$	5 pi	150 A	10 A
14 km	100 %	0.5	0	10 pi	150 A	10 A
28 km	100 %	0.5	0	10 pi	150 A	10 A
14 km	100 %	0.5	0	5 pi	300 A	10 A
28 km	100 %	0.5	0	5 pi	300 A	10 A
14 km	100 %	0.5	0	5 pi	150 A	30 A
28 km	100 %	0.5	0	5 pi	150 A	30 A
14 km	80 %	0.5	0	5 pi	150 A	30 A
28 km	80 %	0.5	0	5 pi	150 A	30 A

Conductor types used in this thesis are AXCEL 3X95/16 and FEAL99. The model for conductors, pi-component, is available at PSCAD’s master library. Only conductor-specific parameters have to be defined. AXCEL 3X95/16 is an underground cable, which was used in Lars Anderssons (Andersson 2005: 8) investigations, and it has electrical parameters shown on the page 53 in the figure 23. It should be noticed that there is possible error in the parameters given in Andersson’s work. Zero sequence inductive reactance has to have bigger value than positive sequence inductive reactance, but they don’t have. At this work zero sequence value is used as positive sequence value and vice versa.

The image shows a software dialog box titled "[pi\_coupled] Coupled pi-section". It contains a list of electrical parameters for a coupled pi-section, each with a corresponding input field. The parameters are organized into two columns: positive sequence (+ seq.) and zero sequence (0 seq.).

Parameter	Value
+ seq. resistance (Ohm/km)	0.32
0 seq. resistance (Ohm/km)	3.92
+ seq. inductance	1.0 [H/km]
+ seq. ind. reactance (Ohm/km)	0.086
0 seq. inductance	1.1 [H/km]
0 seq. ind. reactance (Ohm/km)	0.092
+ seq. capacitance	0.302 [uF/km]
+ seq. cap. susceptance	1.1 [uS/km]
+ seq. cap. reactance (Ohm*km)	1.0
0 seq. capacitance	0.301 [uF/km]
0 seq. cap. susceptance	1.0 [uS/km]
0 seq. cap. reactance (Ohm*km)	1.1

At the bottom of the dialog box, there are three buttons: "OK", "Cancel", and "Help...".

**Figure 23.** Electrical parameters of AXCEL 3X95/16 underground cable.

FEAL99 is a typical overhead line conductor, which is made of iron and aluminium. It has electrical parameters shown on the page 53 in the figure 24.

Parameter	Value
+ seq. resistance (Ohm/km)	0.33
0 seq. resistance (Ohm/km)	0.48
+ seq. inductance	1.0 [H/km]
+ seq. ind. reactance (Ohm/km)	0.39
0 seq. inductance	1.1 [H/km]
0 seq. ind. reactance (Ohm/km)	1.94
+ seq. capacitance	0.006 [uF/km]
+ seq. cap. susceptance	1.1 [uS/km]
+ seq. cap. reactance (Ohm*km)	1.0
0 seq. capacitance	0.005 [uF/km]
0 seq. cap. susceptance	1.0 [uS/km]
0 seq. cap. reactance (Ohm*km)	1.1

**Figure 24.** Electrical parameters of FEAL99 overhead line.

The duration of each simulation run is 0,35 seconds. Fault initiates at the time of 0,15 seconds. Measurements for the healthy state are scheduled to be made at the time of 0,1 seconds and measurements for the faulty state are scheduled to be made at the time of 0,3 seconds. A 50  $\mu$ s simulation time step is going to be used for all simulation runs.

## 5.2. Network modeled by PSCAD

Studied network consists of a three-phase voltage source, the studied feeder and the background network. The adjustable Petersen coil and parallel-connected resistance are connected to the neutral point of the voltage source. Parameters of the Petersen coil model are shown on the page 55 in the figure 25.

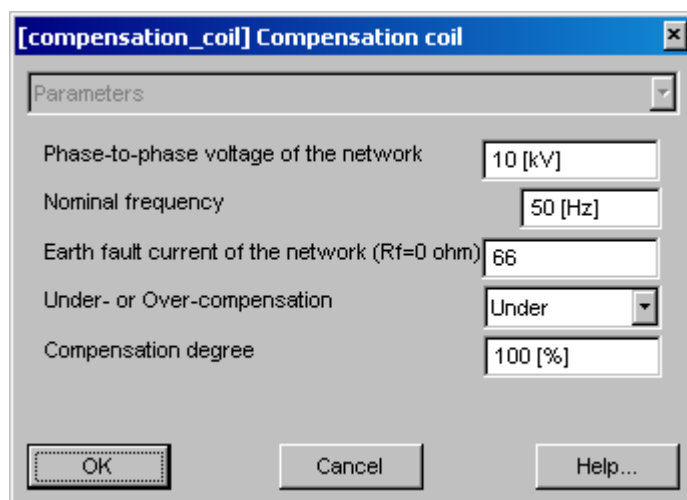


**Figure 25.** Settings of Petersen coil model.

In the simulations, the compensation degree and earth fault current as a function of network size are varied. Correct value for the coil inductance is calculated from these values. Petersen coils parallel resistance is determined by desired current value and voltage over the resistance. Parameters for resistance are shown in the figure 26.

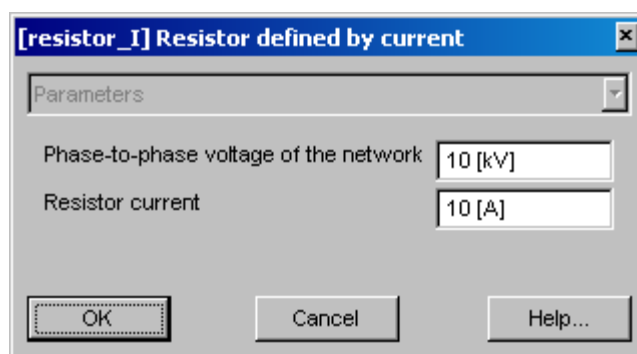


**Figure 26.** Settings of Petersen coils parallel resistance.

In the figures 27 and 28, the two types of networks, which are used at simulations, are shown. The first figure shows the network, which is used for most of the simulations.

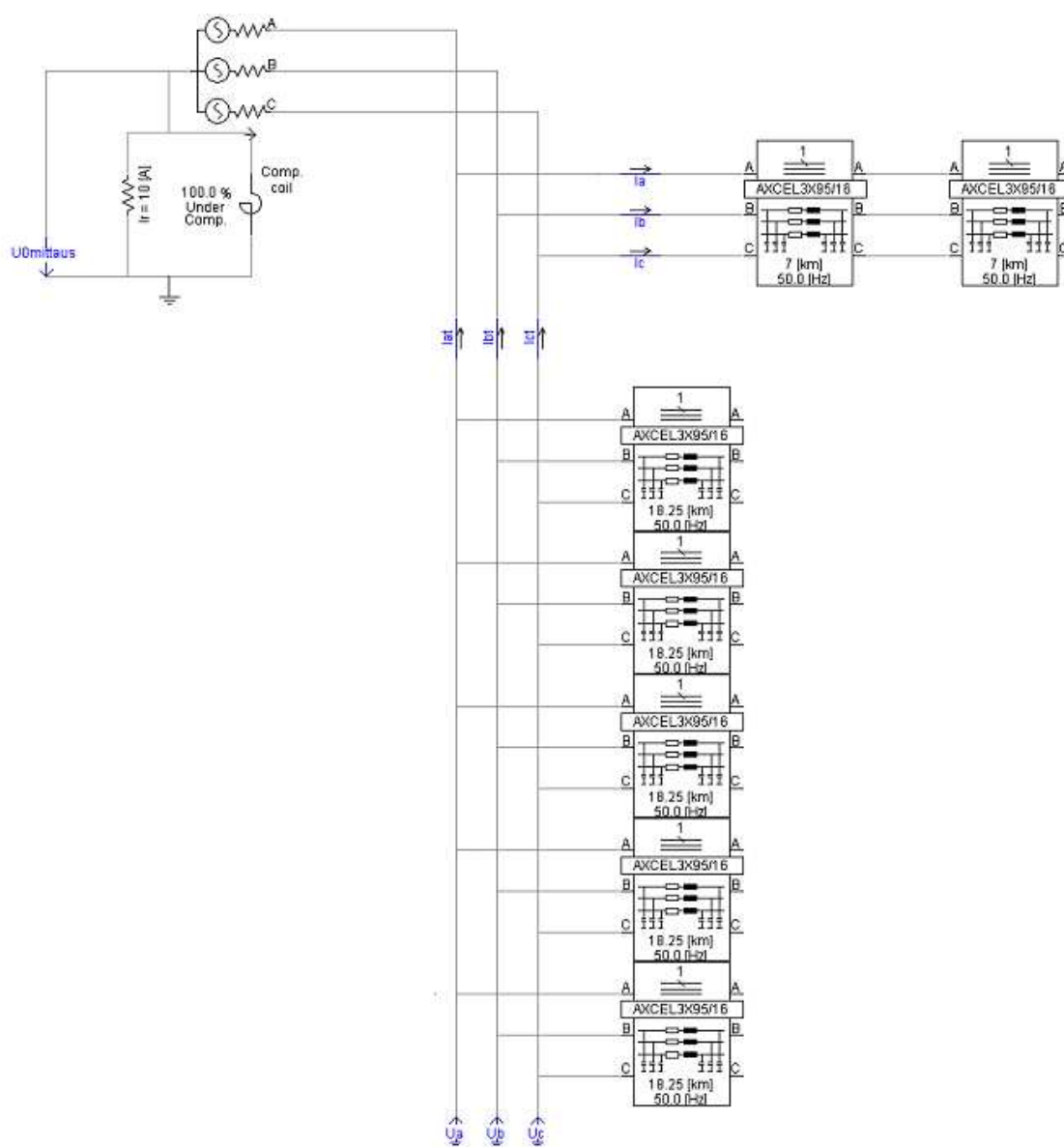


**Figure 27.** PSCAD model used in most of the simulations.

The second figure shows the network, which is used to examine the effect of some cable length divided to the larger number of feeders of the background network. This may affect the fault currents.



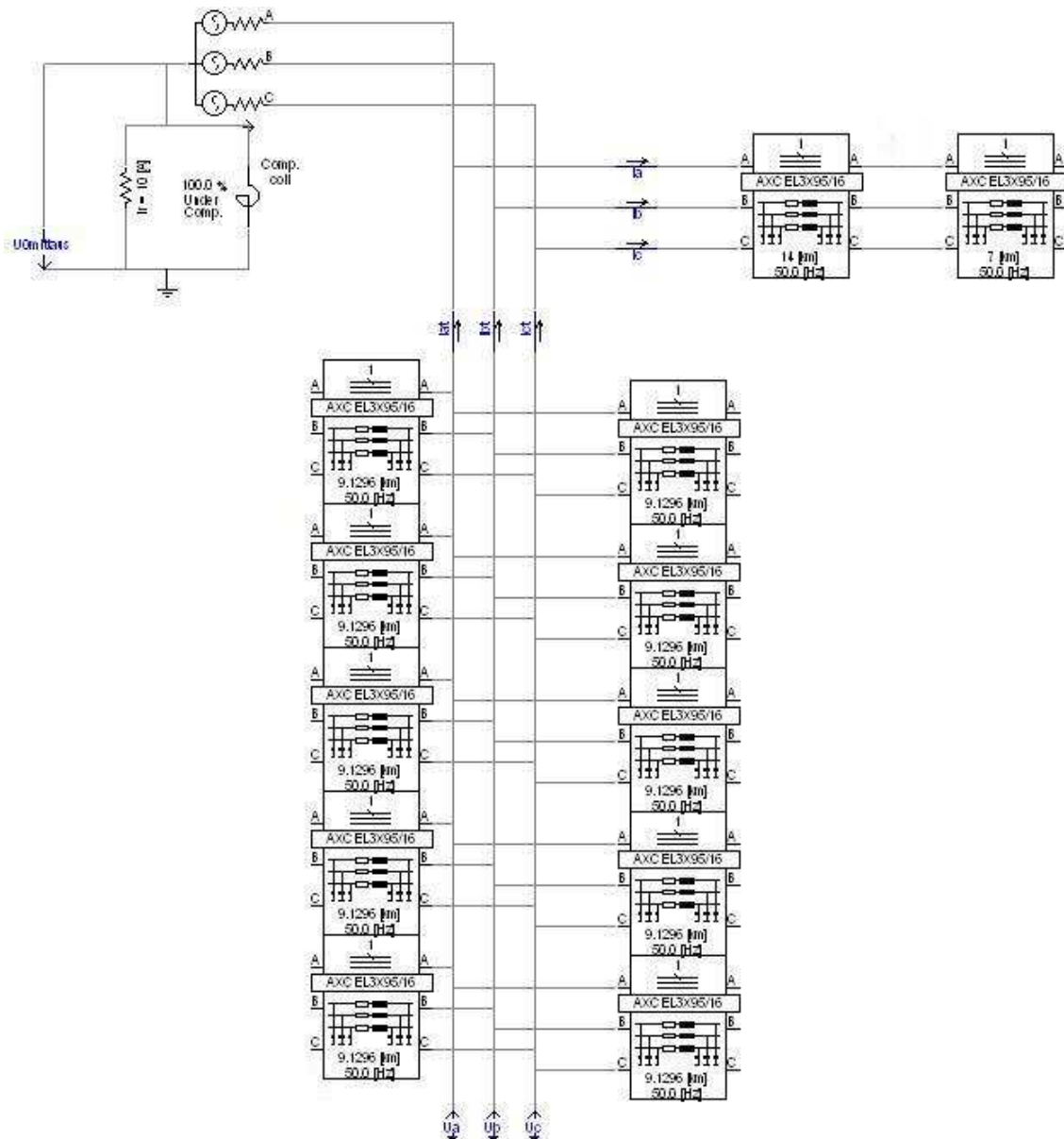


**Figure 28.** PSCAD circuit, which is used to test effect of larger amount of cable feeders in the background network.

### 5.3. Simulation data and Matlab® script

When PSCAD simulations are carried out, the output files containing the results are created in the same folder with the actual PSCAD model. The output files are plain text files, which contain all the data provided by the data channels, which have been in use

at the simulation model. The data is read by a Matlab® script, which reads phase currents and voltages from output files and then calculates zero sequence values. These zero sequence values are then processed with Fourier transform filter. It gives phasor values of 50 Hz component of zero sequence values zero sequence current  $I_{0df}$  and zero sequence voltage  $\underline{U}_{0df}$ . The Matlab® code, which calculates the quantities monitored by the protection functions, is presented in Appendix 1. Rough block diagram of the script is shown in the figure 29.

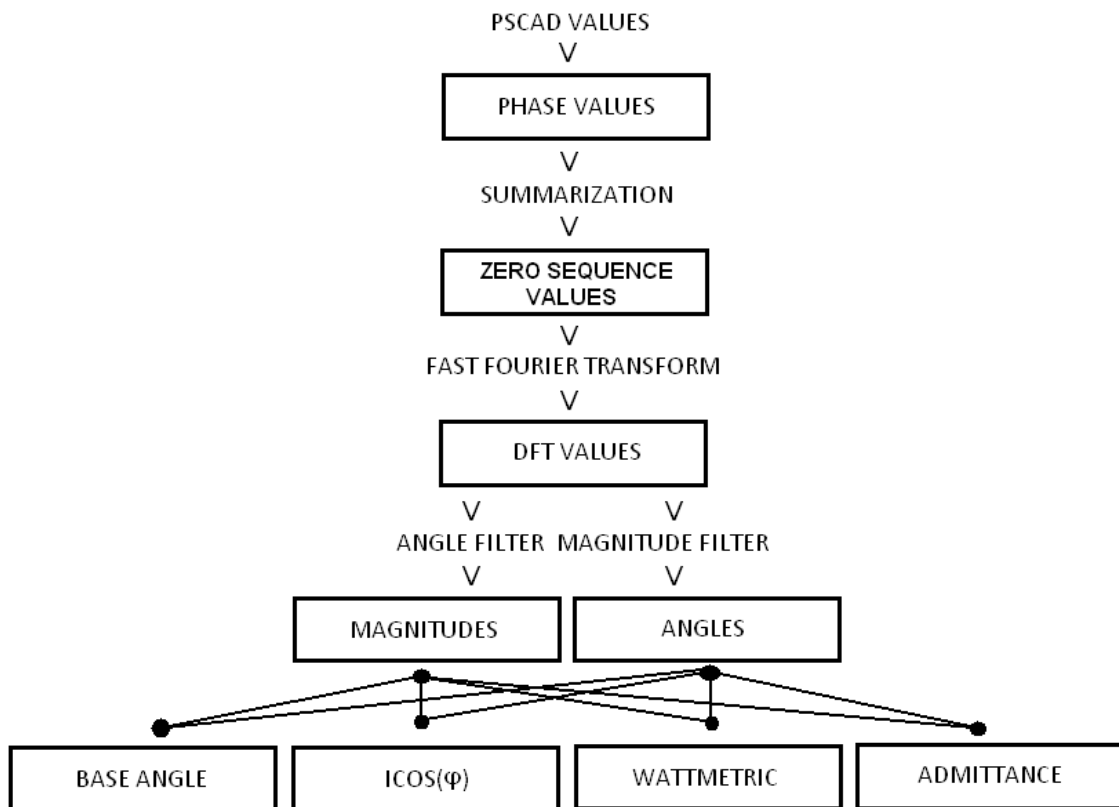


**Figure 29.** Block diagram showing roughly how Matlab® script works.

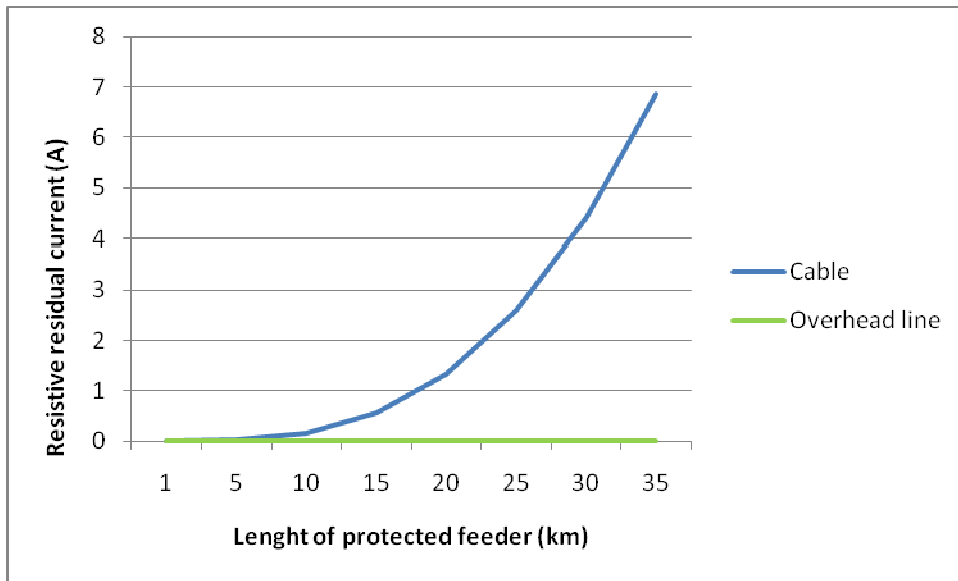
## 6. SIMULATIONS

Due to the large amount of simulation data, only the essential results are shown. Charts and figures show the most important results. Less important and obvious results are only mentioned at the text. All the simulation results are available in Appendix 2. In the results, three different numbers indicate the fault location. 0 indicates that the fault is in the beginning of the studied feeder, 0.5 indicates fault at the middle of the feeder, and 1 indicates fault at the end of the feeder. At the beginning it is needed to verify that Jussi-Pekka Pouttu's and Lars Andersson's conclusions are possible to repeat.

### 6.1. Verification of the non-linear increase of resistive fault current as a function of cable length

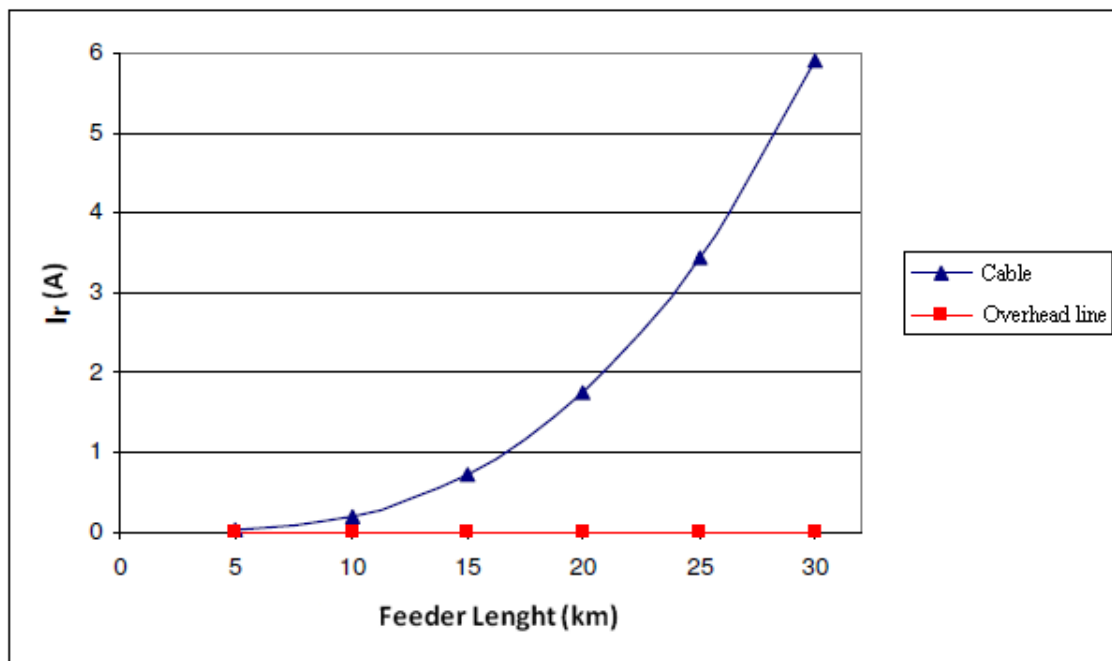
To verify the observation given in reference (Andersson 2005: 13) – the non-linear behaviour of the fault current as a function of cable length - an additional simulation was made. The simulation was conducted with a network model, where the background network is 400 km long FEAL99 overhead line network, consisting of 4 different 100 km pi-sections in parallel. Studied feeder was built by FEAL99 overhead line or AXCEL 3X95/16 cable. Length of the studied feeder was varied from 1 km to 35 km by 5 km steps. The Petersen coil was tuned to 80 % compensation level and parallel resistance of the coil was switched on all the time. The resistor is set to produce negligible resistive current, because only the resistive current produced by the cables is wanted to be seen. Voltage level of the network was 10 kV. To prove that, at the long cable feeder, the resistive fault current increases in an exponential fashion as function of cable length, it is necessary to measure currents in the case when the earth fault occurs in reverse direction i.e. outside the protected feeder.

Figure 30 shows how resistive current's magnitude acts when fault occurs outside the protected feeder i.e., in the background network.



**Figure 30.** Resistive component of the residual current when measurements are carried after the fault i.e. fault is in the background network.

Lars Andersson similar result (Andersson 2005: 13) is shown in the figure 31.



**Figure 31.** Resistive component of a fault current as a function of cable length (Andersson 2005:13).

Since both figures 30 and 31 are equal, it is proved that result of Andersson's and Pouttu's thesis can be repeated and result given by the model applied are valid.

## 6.2. Base angle criterion

At the base angle criterion, zero sequence voltage  $\underline{U}_0$  and zero sequence current  $\underline{I}_0$  were measured. In all situations when the network is in healthy state, zero sequence voltage  $\underline{U}_0$  was near zero. This is due to the fact that network was modeled as symmetrical i.e. natural asymmetry that causes non-zero healthy state zero sequence values was neglected. When a solid, zero resistance, earth fault occurred, zero sequence voltage increased to value of phase voltage, reaching maximum voltage of 6332 V. Higher fault resistance gave lower zero sequence voltage. Highest zero sequence voltage values were measured, when network is operated near full resonance.

Zero sequence currents measured at beginning of the protected feeder during an earth fault inside the protected feeder increased when network size increased. The highest value of zero sequence current was measured when compensation level was 120 %. This current peaked to 51.85 A.

The first clear issue of angle information was, that current's angle moved clockwise in the complex plane when the studied feeder length increases. The second clear issue was that every simulated fault case in the studied feeder gave fault current vector within  $\pm 90$  degrees range from the reference voltage vector. More information can be viewed from the following nine figures. It seems that total compensation couldn't be reached in the model even if Petersen coil was exactly tuned, and that perfect tuning cannot be ever reached in reality either. Network model had to be driven a bit over-compensated to get 100 % compensation. This can be seen from Appendix 2, where all the values got from the simulation are shown. All the zero sequence current vectors are shown at the following nine figures. Voltage vector shows only a direction of zero sequence voltage  $-\underline{U}_0$ , magnitude of this vector is set to a arbitrary value. Direction of the zero sequence voltage  $-\underline{U}_0$  was chosen so that the figures correspond to the relay characteristic shown in

figure 19 on the page 40. When the real part of the current vector is positive, the fault is at the studied feeder.

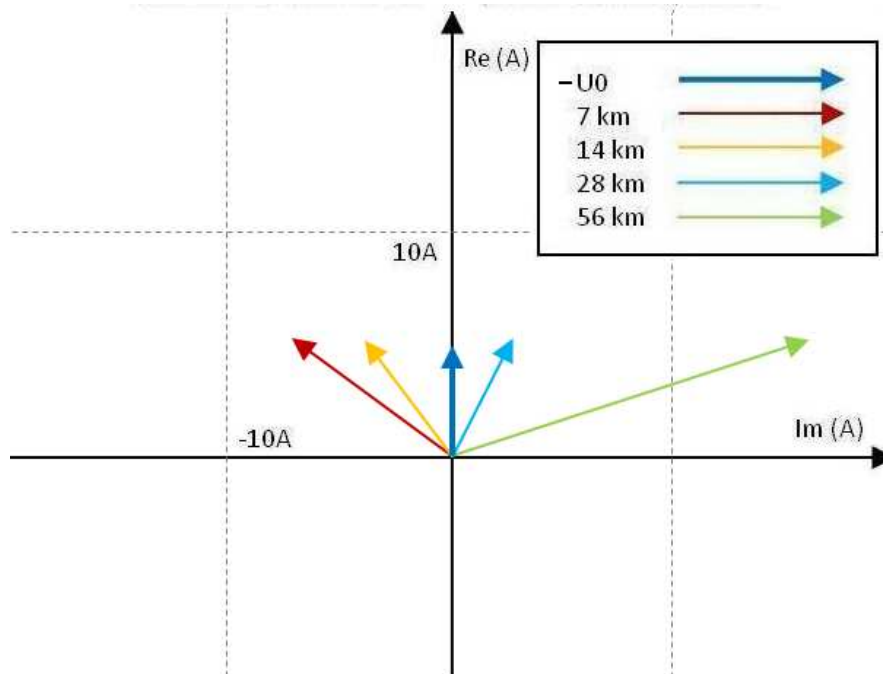


**Figure 32.** Zero sequence current values with 80 % compensation and fault location 0.

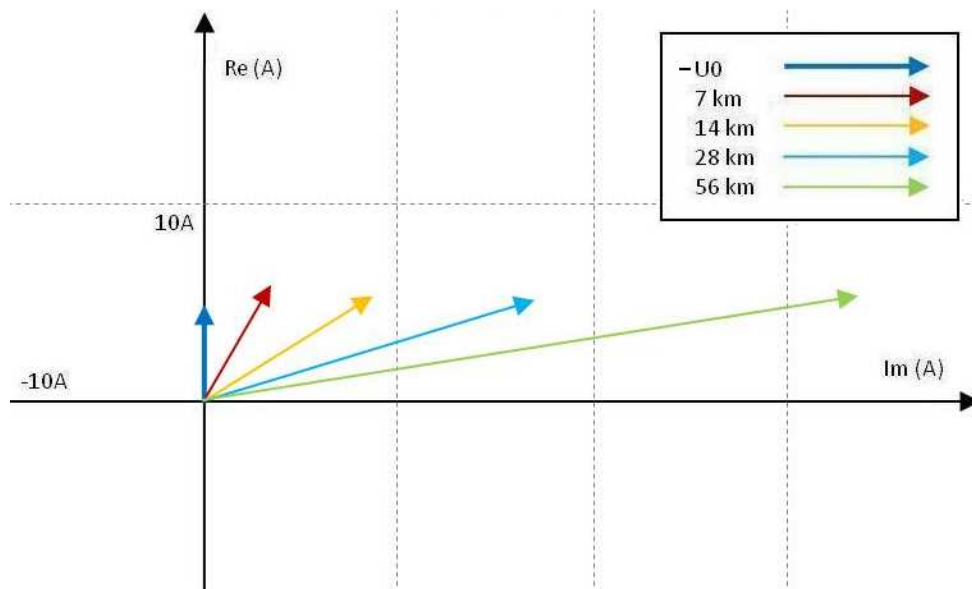


**Figure 33.** Zero sequence current values with 100 % compensation and fault location 0.

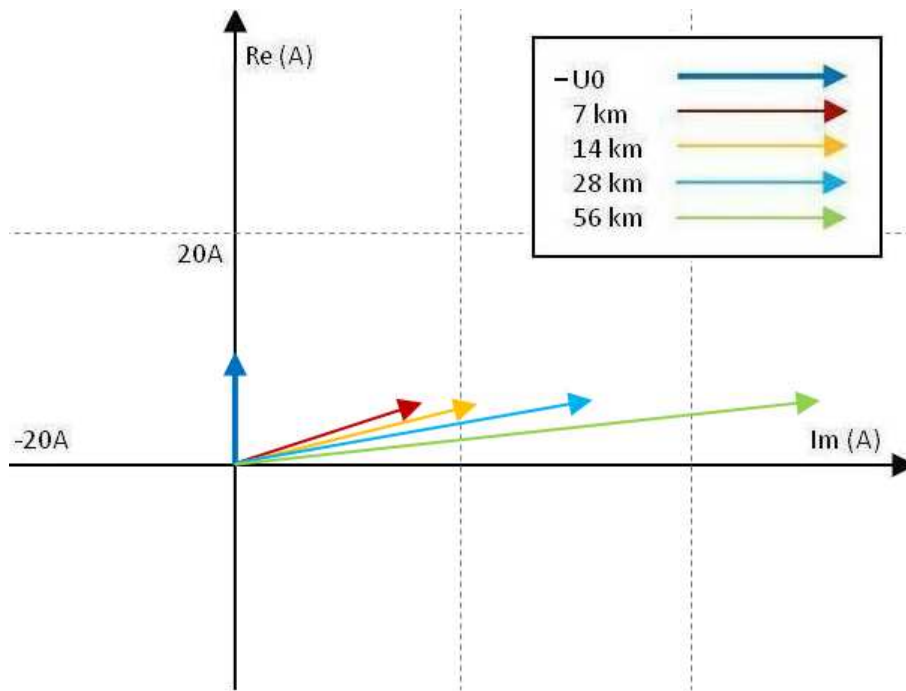


**Figure 34.** Zero sequence current values with 120 % compensation and fault location 0.

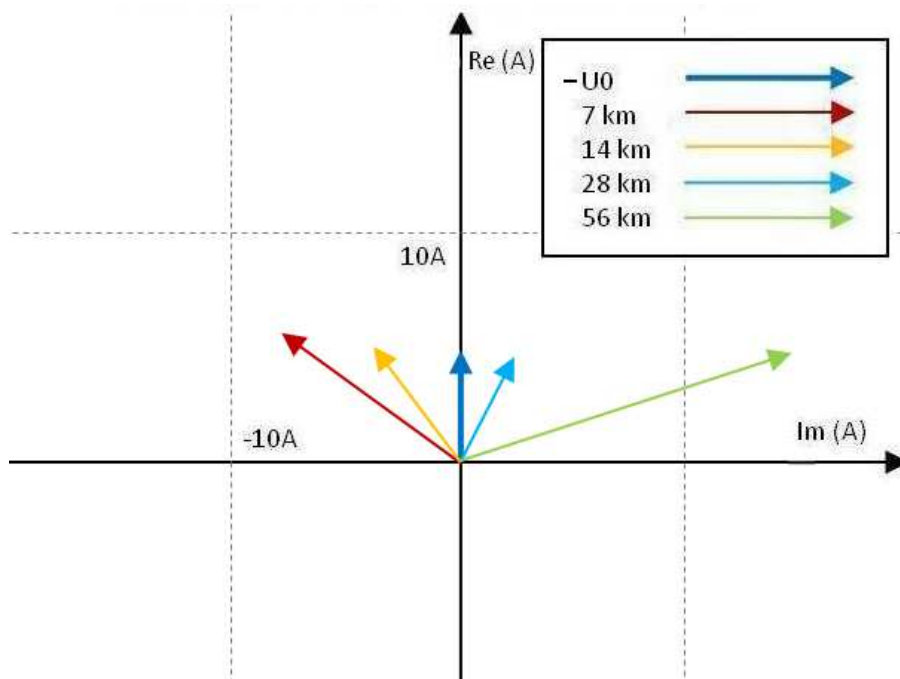


**Figure 35.** Zero sequence current values with 80 % compensation and fault location 0.5.

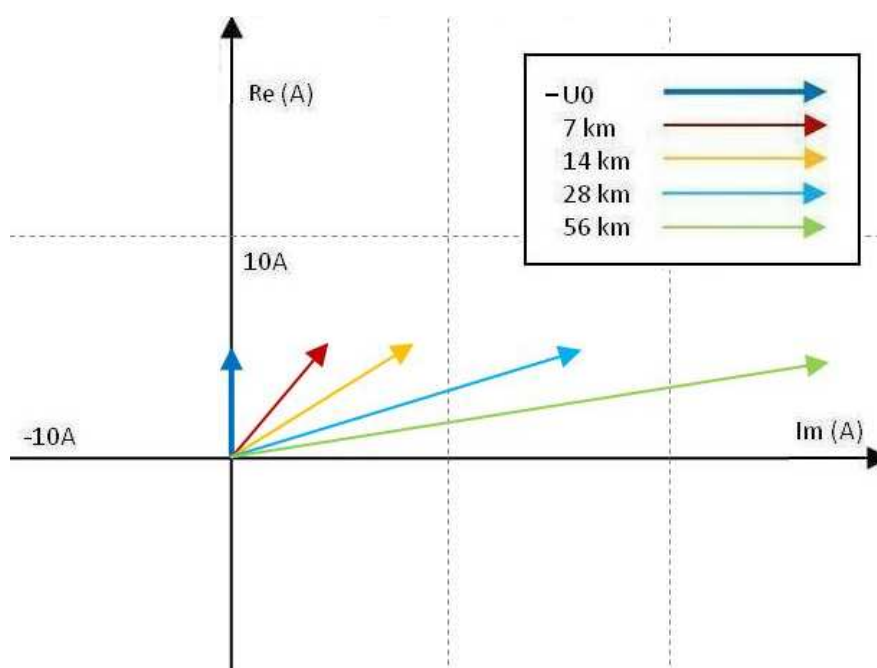


**Figure 36.** Zero sequence current values with 100 % compensation and fault location 0.5.

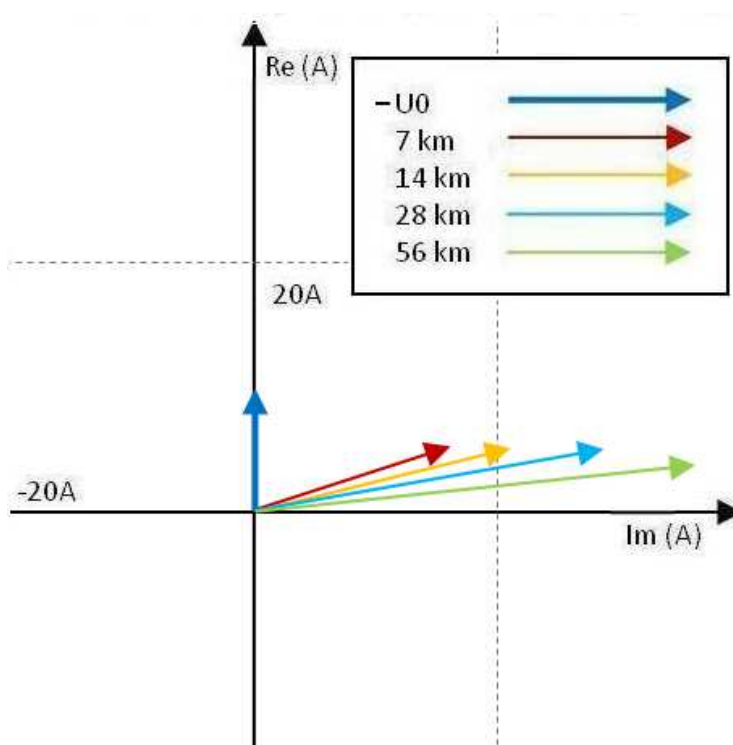


**Figure 37.** Zero sequence current values with 120 % compensation and fault location 0.5.



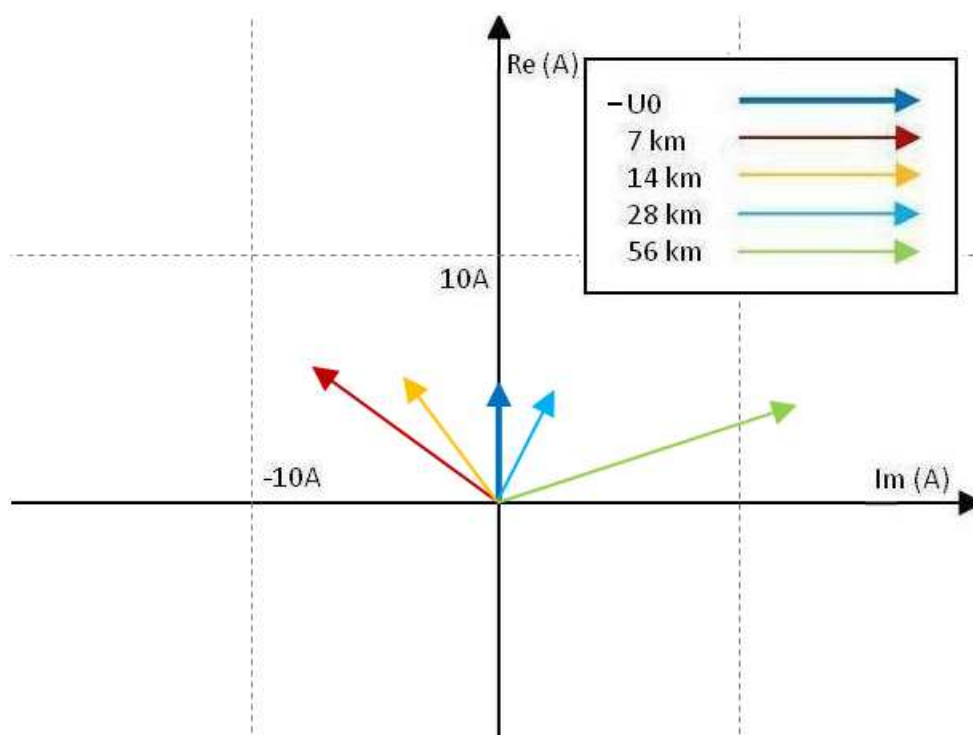


**Figure 38.** Zero sequence current values with 80 % compensation and fault location 1.

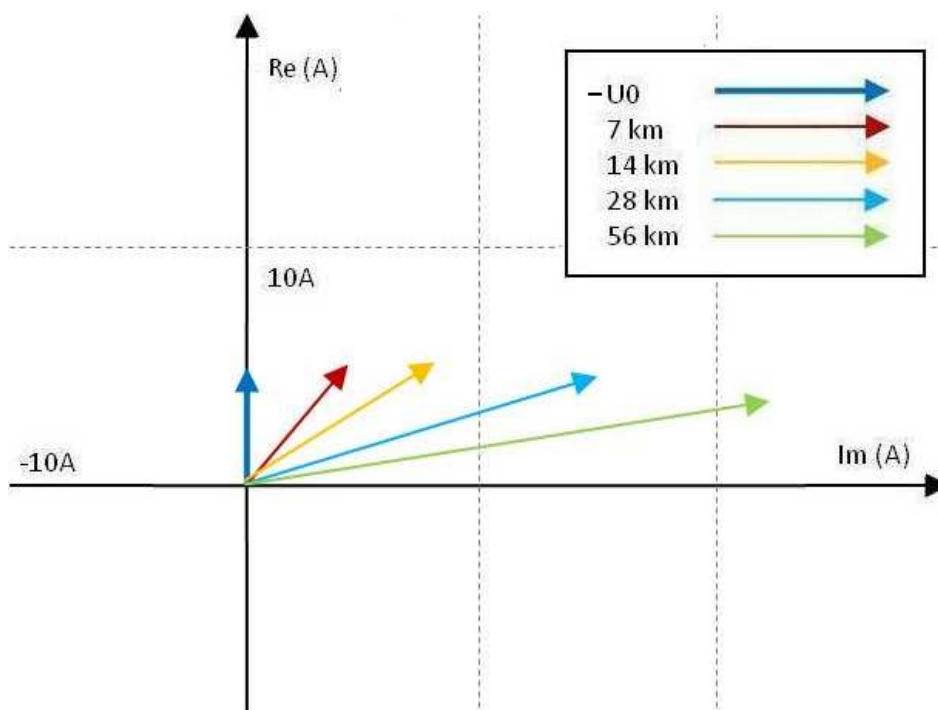


**Figure 39.** Zero sequence current values with 100 % compensation and fault location 1.

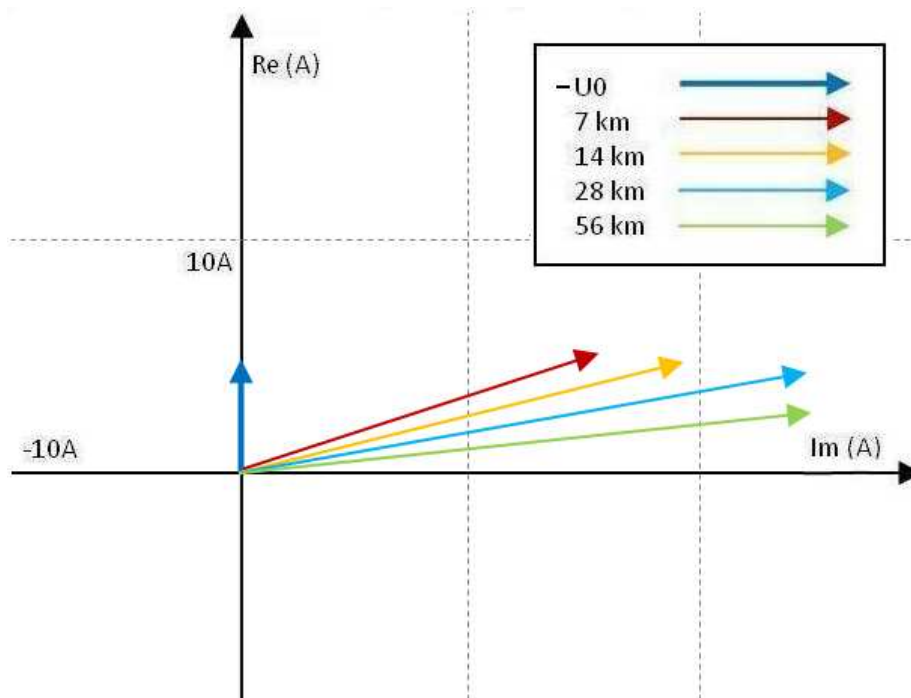


**Figure 40.** Zero sequence current values with 120 % compensation and fault location 1.

The special case simulation results are presented on the page 67 in the figure 41. At these simulations fault location was middle of the studied feeder and compensation level was 100 %. When fault occurred at the background network, the angle moves in totally other direction, and clearly showed that the fault was not at the studied feeder. This result can be verified from the Appendix 1.

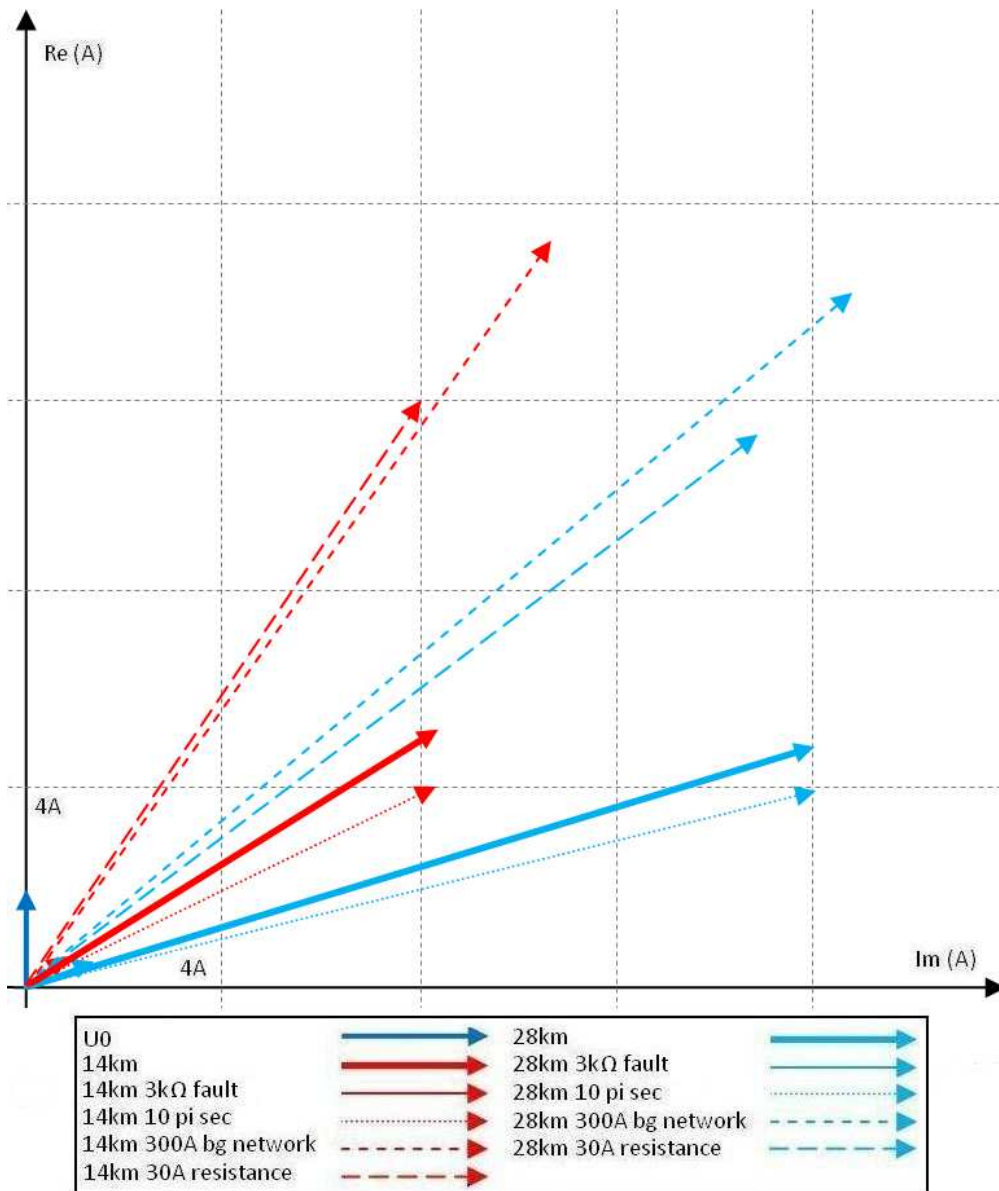


**Figure 41.** Zero sequence current values at special cases.

In the figure 41 acronym “10 pi sec” stands for the number of pi-section models in the background network’s feeders and “bg” stands for background.

### 6.3. $I_0\cos(\varphi)$ protection method

In  $I_0\cos(\varphi)$  protection method, zero sequence current’s magnitude and angle information were used. It indicates the resistive current flow at the measuring point. Values which

$I_0\cos(\varphi)$  gave were as expected. When the fault occurred at the beginning of the studied feeder,  $I_0\cos(\varphi)$  reached nearly same current value which didn't depend on the length of the studied feeder. When the fault occurred at the middle point of the studied feeder, the value of the  $I_0\cos(\varphi)$  decreased the longer the studied feeder was. The value decreased also, when the fault occurred at the end of studied feeder. Systematically measured  $I_0\cos(\varphi)$  values are shown in the two following figures.

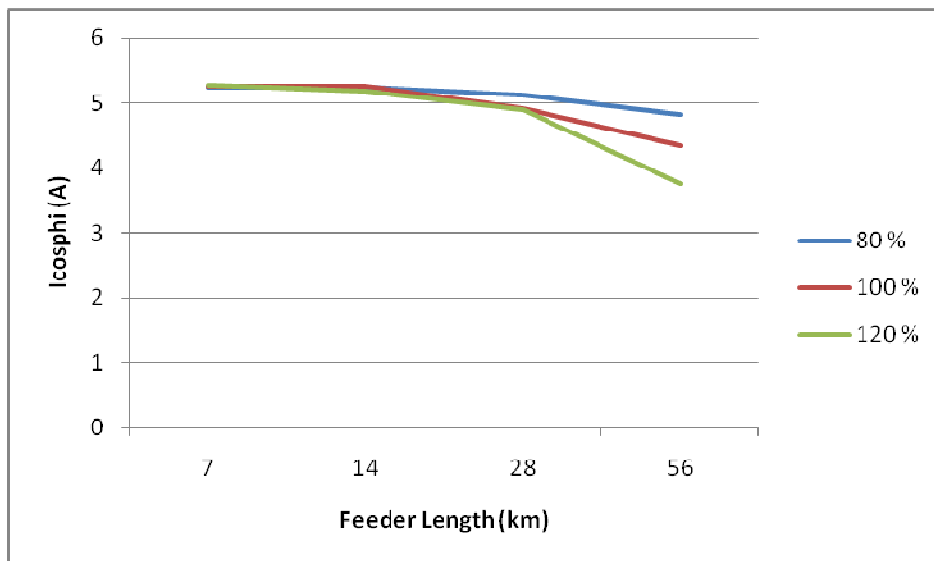


**Figure 42.**  $I_0\cos(\varphi)$  values in fault location 0.5.

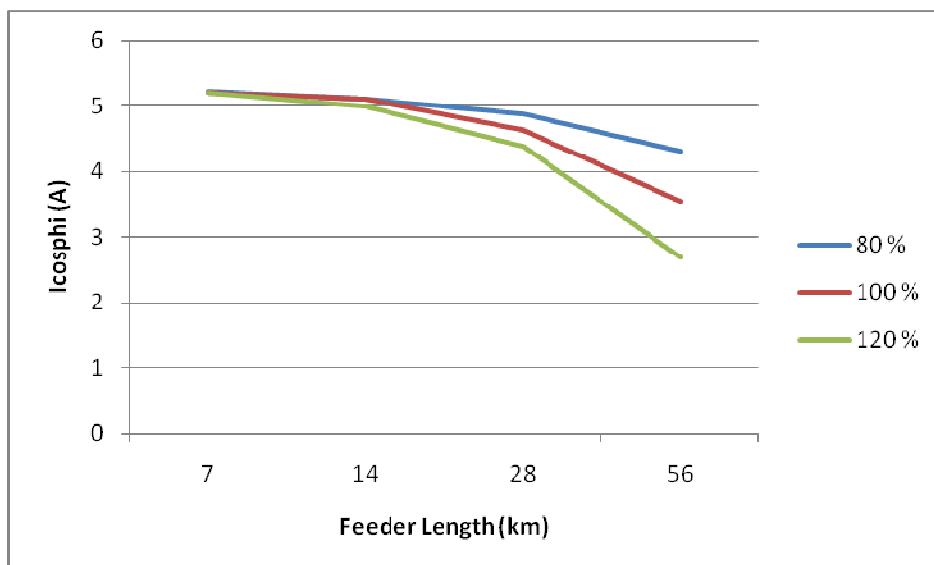


**Figure 43.**  $I_0\cos(\varphi)$  values in fault location 1.

Special case measurements showed interesting results. It was surprising that when the background network current value was doubled, the fault current nearly tripled. Only little surprising was change at the values when background network was changed from 5 pi-sections to 10 pi-sections, even though the length of the background network remained equal.

When high resistance earth faults are tried to cope with, it was a very good idea to introduce smaller Petersen coil's parallel resistance to allow higher resistive current flow at the network. Simulations proved that, when the current value of the parallel resistance was tripled from 10 A to 30 A, the fault current increased, but the increase is smaller when the protected feeder is longer. Smaller parallel resistance was not introduced in the situation of 3 k $\Omega$  fault, but it is obvious that the ability to detect such faults will certainly improve. Special case measurements are shown in the following two figures.

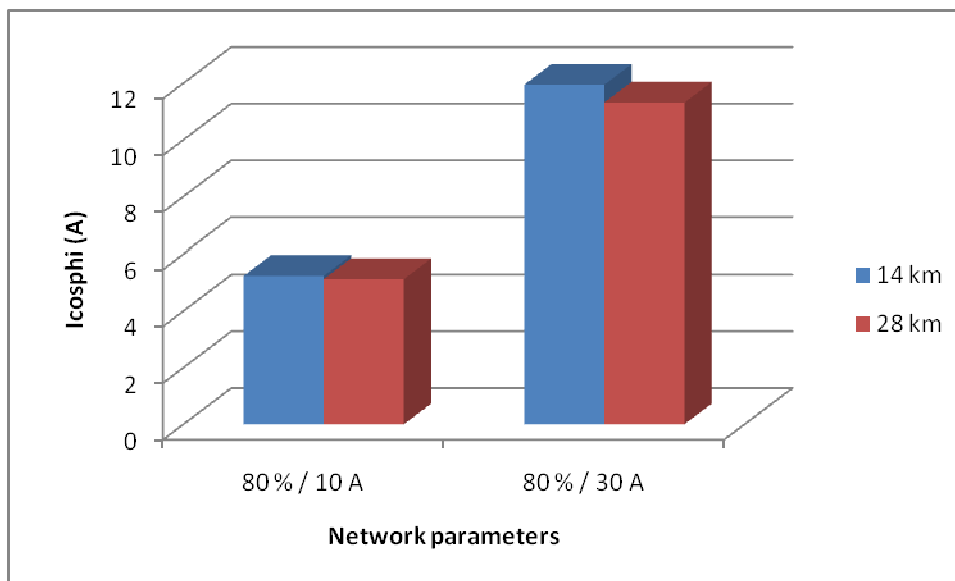


**Figure 44.** Comparison between different sized parallel resistors at 80 % compensation level and in the fault location 0.5.

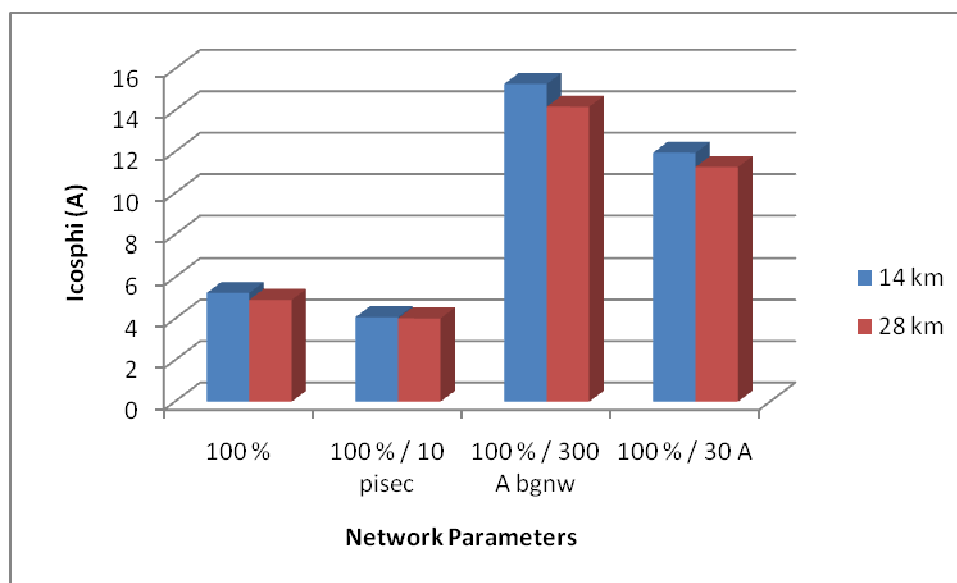


**Figure 45.** Comparison between normal case and special cases at the 100 % compensation level and in the fault location 0.5.

In the figure 45, the acronym “10 pise” stands for the number of pi-section models in the background network feeders and “bgnw” stands for background network.

#### 6.4. Wattmetric protection method

In Wattmetric protection procedure, the active power was measured. All the information that was needed in the base angle criterion is also used here. All the Wattmetric values were somewhat same with the  $I_0\cos(\varphi)$  values. When the fault was at the beginning of the feeder, the length of the studied feeder didn't affect on Wattmetric value. The higher the level of compensation was, the smaller the change in Wattmetric value was, when the length of the studied feeder increased. All measurements are shown in the following two figures.

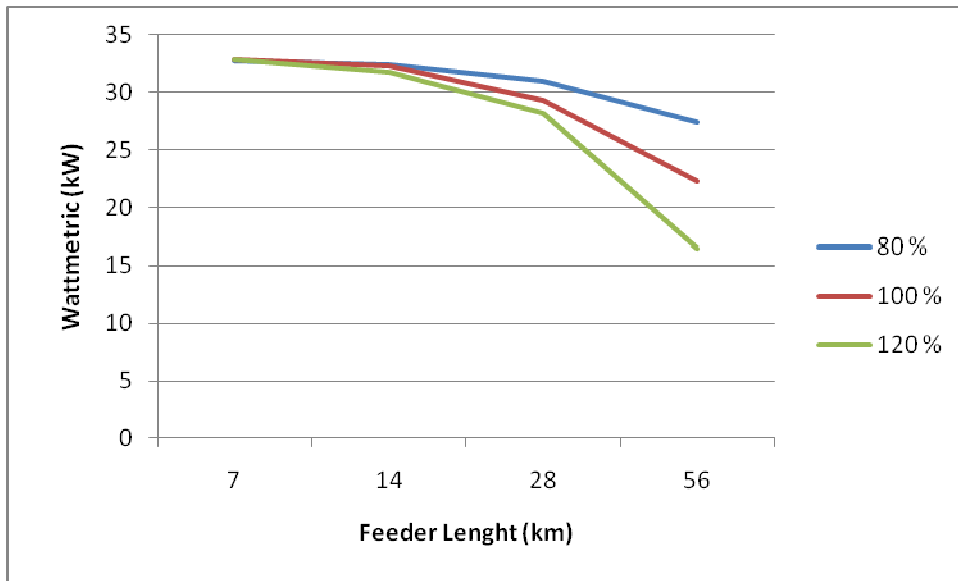


**Figure 46.** Wattmetric values in fault location 0.5.

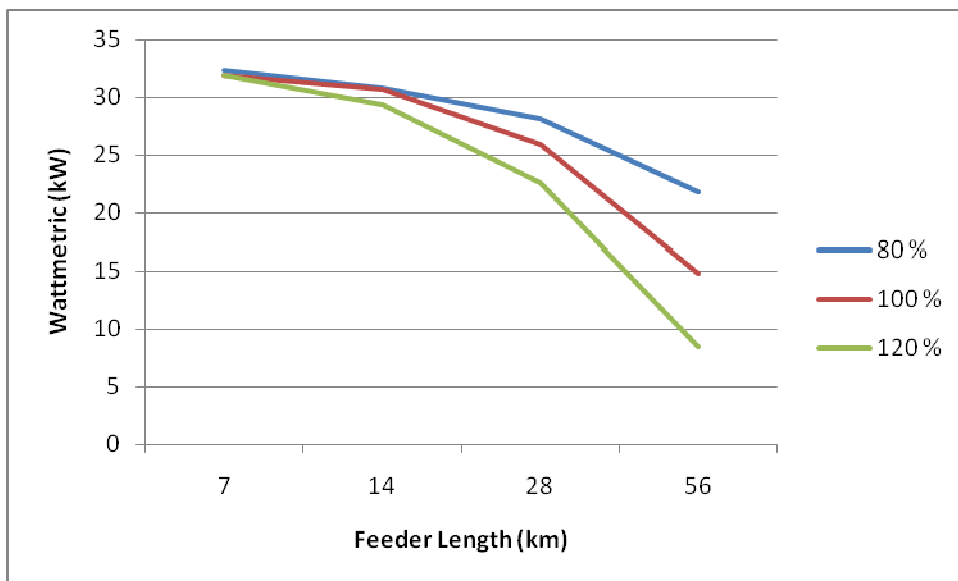


**Figure 47.** Wattmetric values in fault location 1.

In the special cases, the same trend could be seen as it were seen in  $I_0 \cos(\varphi)$  values. Decreasing the value of parallel resistance of Petersen coil makes detection of faults, especially high resistance faults, much easier. Other values also indicated same sort of behaviour which was seen in  $I_0 \cos(\varphi)$  values. Special case measurements are shown in the following two figures.

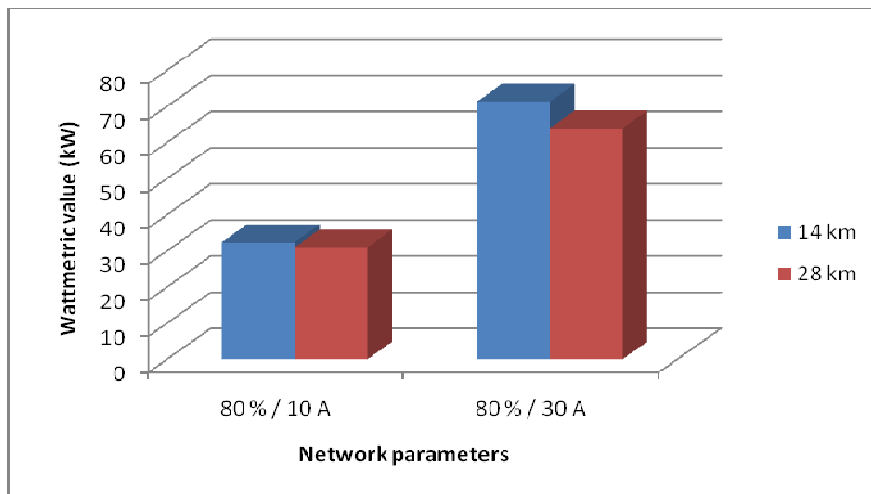


**Figure 48.** Comparison between different sized parallel resistors at 80 % compensation level and in the fault location 0.5.

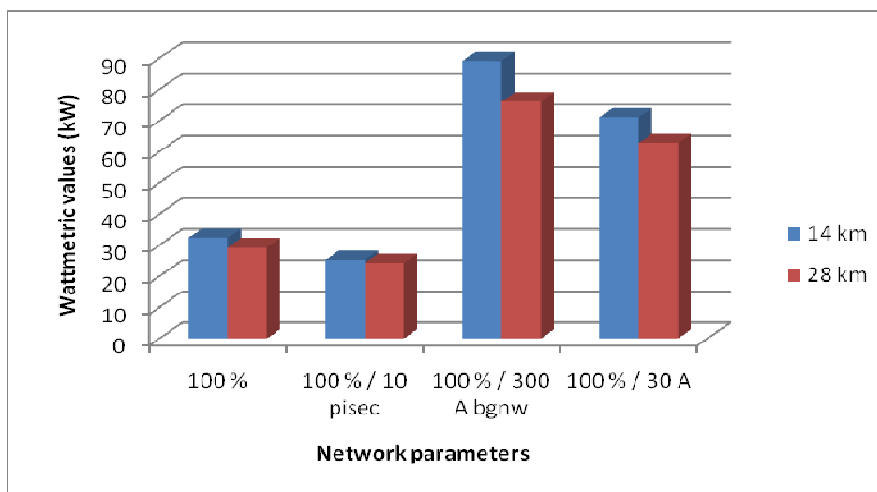


**Figure 49.** Comparison between normal case and special cases at the 100 % compensation level and in the fault location 0.5.

In the figure 49 the acronym “10 pisecc” stands for the number of pi-section models in the background network feeders and “bgnw” stands for background network.



### 6.5. Neutral Admittance protection method

Neutral Admittance method relied on the division between zero sequence current and zero sequence voltage vectors. This division is made by two complex values, and this complex value is then presented in the complex plane. All the simulations results had similar pattern. Systematically, admittance values fell into the fourth quadrant when the fault occurred in the studied feeder. It seems that neutral admittance protection has a lot to give for earth fault protection in large cable networks. The results are shown in the following nine figures.

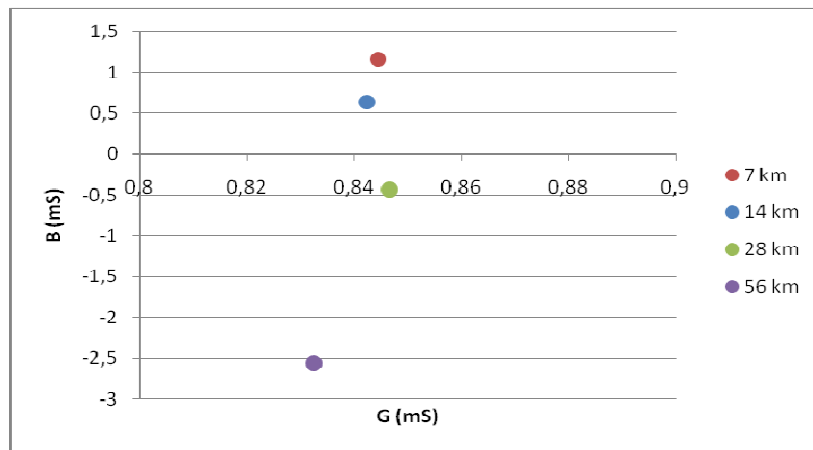


**Figure 50.** Admittance values with 80 % compensation and fault location 0.

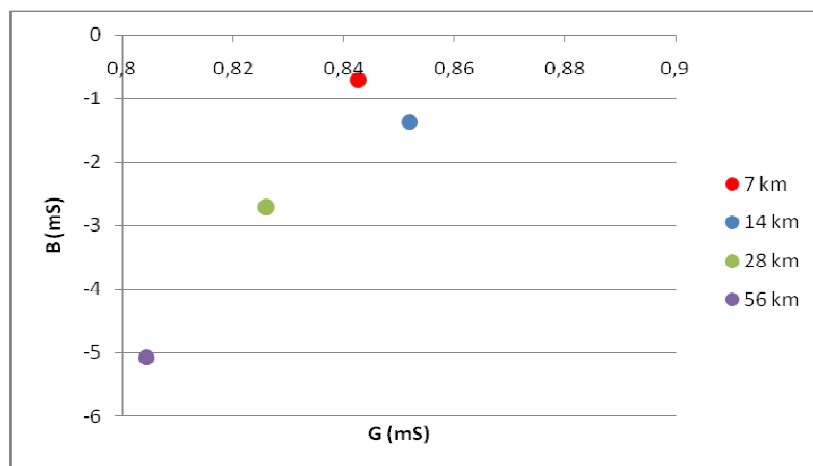


**Figure 51.** Admittance values with 100 % compensation and fault location 0.

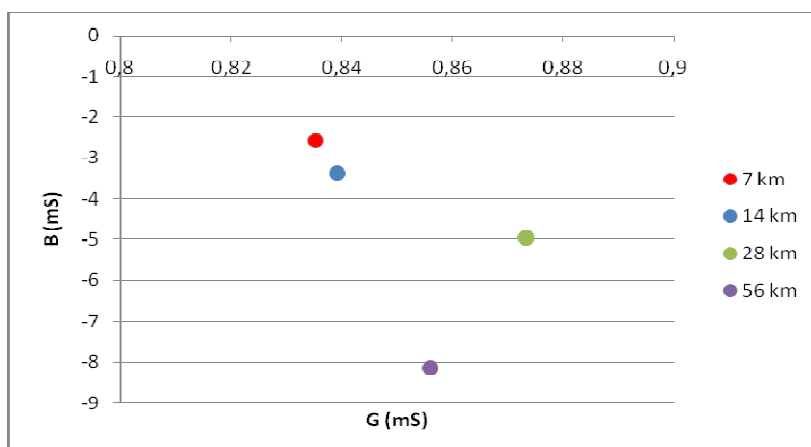


**Figure 52.** Admittance values with 120 % compensation and fault location 0.

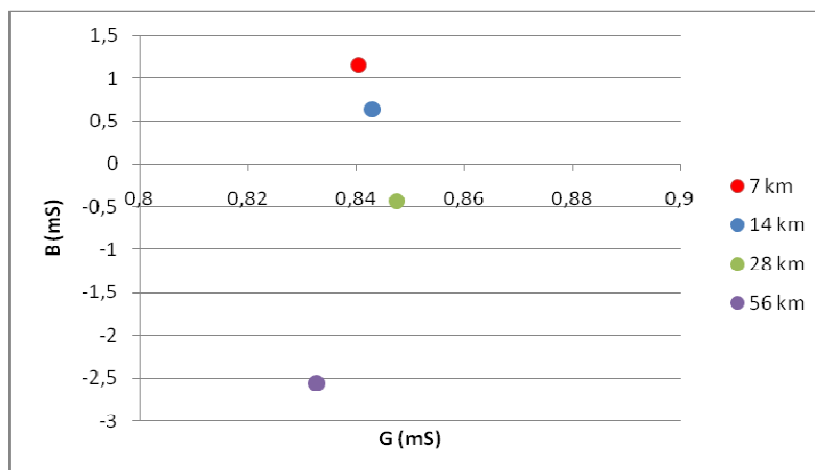


**Figure 53.** Admittance values with 80 % compensation and fault location 0.5.

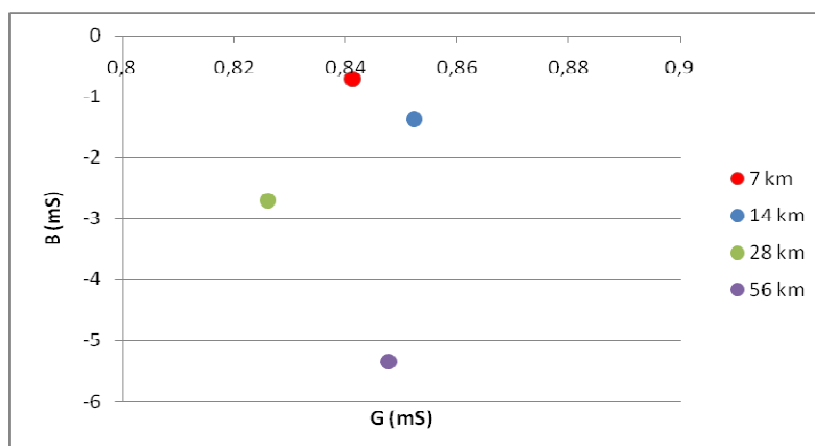


**Figure 54.** Admittance values with 100 % compensation and fault location 0.5.

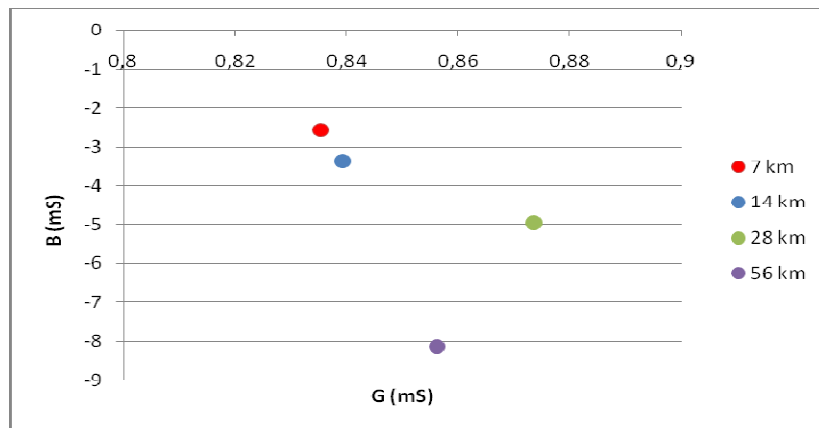


**Figure 55.** Admittance values with 120 % compensation and fault location 0.5.

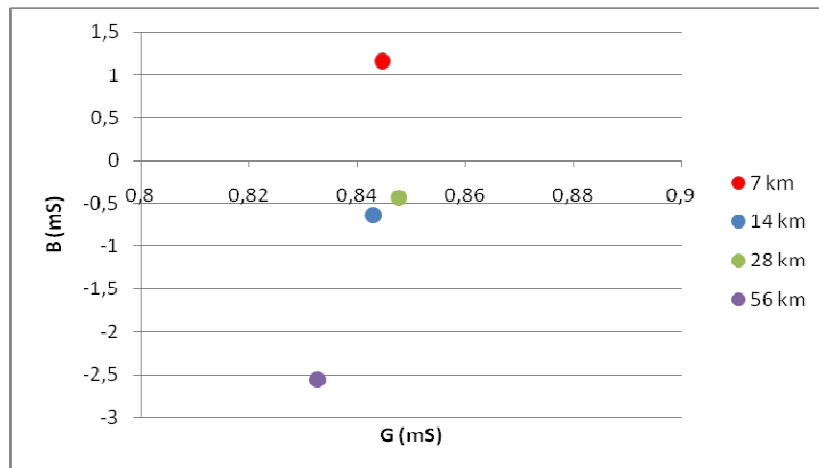


**Figure 56.** Admittance values with 80 % compensation and fault location 1.

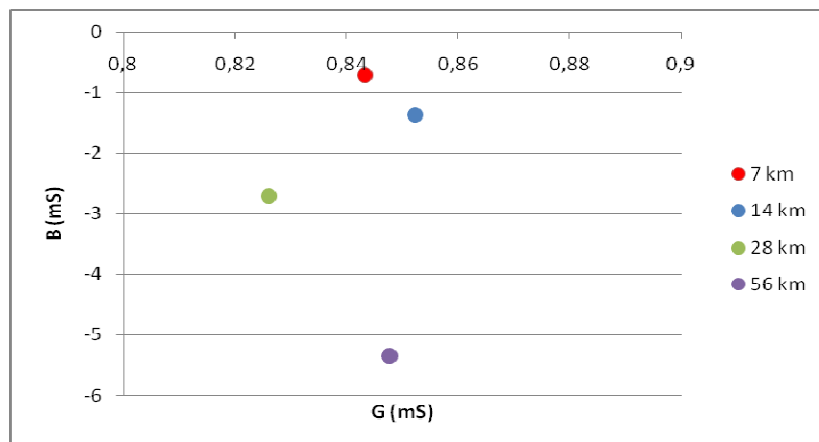


**Figure 57.** Admittance values with 100 % compensation and fault location 1.

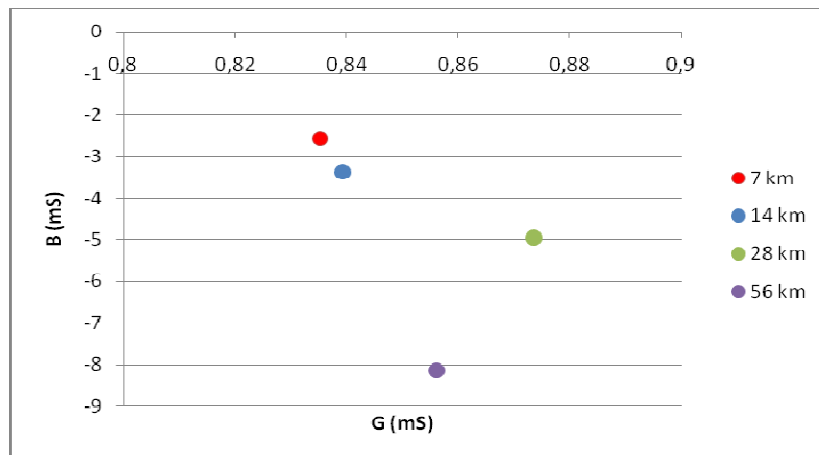


**Figure 58.** Admittance values with 120 % compensation and fault location 1.

Good results were also gained at the special case simulation presented in the following 5 figures. When the fault occurred at the background network shown in figure 59, admittance value was on an other quadrant than in cases where the fault was in the protected feeder. In the results, there was no difference between 80 % and 100 % compensation degree. The only difference was in the lengths of the protected feeder. When the fault came on, both compensation degrees gave similar results with the same feeder lengths. This makes it possible to detect if the fault is in the studied feeder or not.

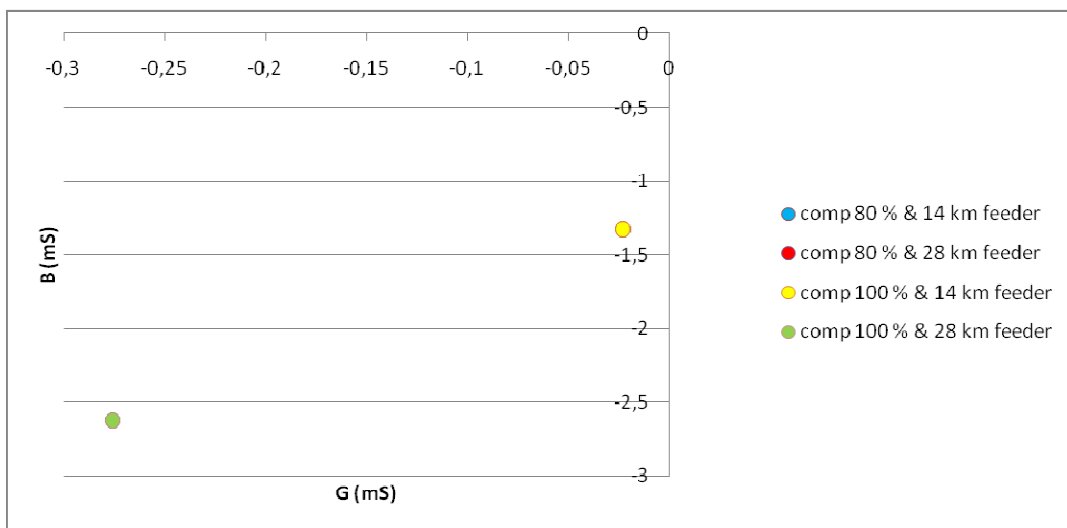


**Figure 59.** Admittance values when fault exists at the background network.

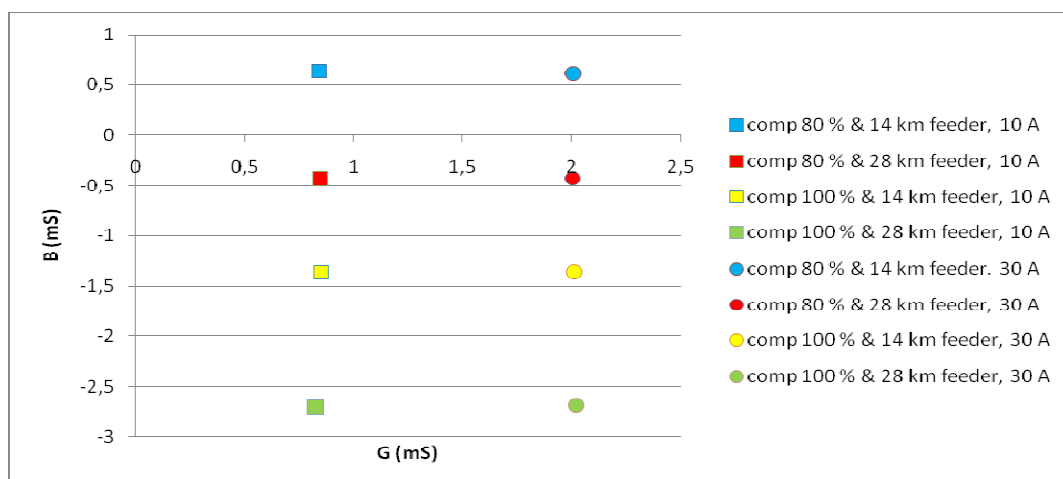


**Figure 60.** Admittance values when current value of Petersen coils parallel resistance is tripled.

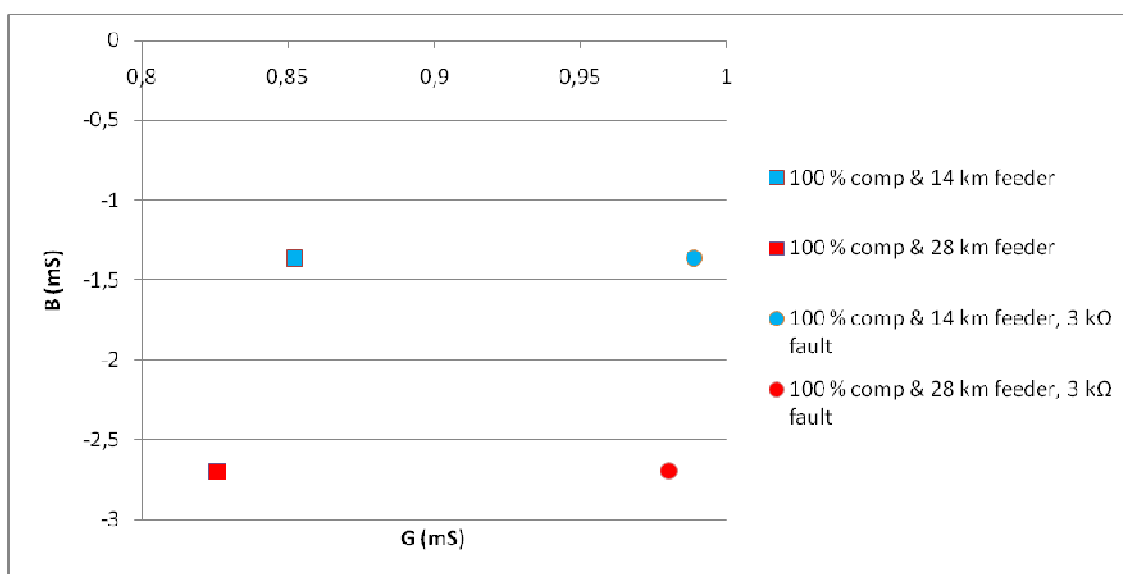


**Figure 61.** Admittance values at 3 kΩ earthfault.

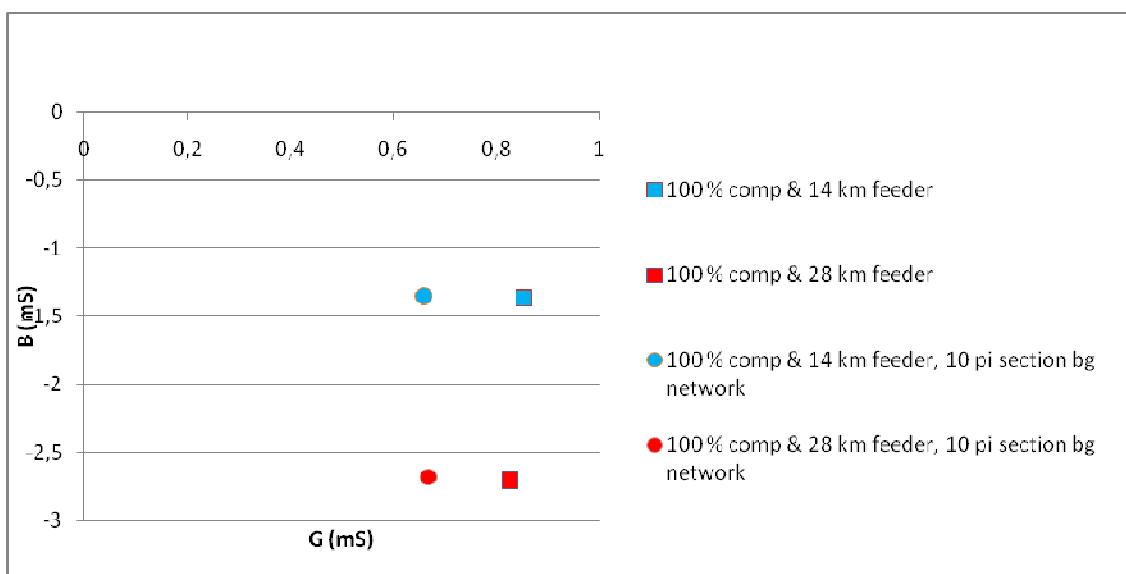


**Figure 62.** Admittance values when background network is made by 10 pi sections.

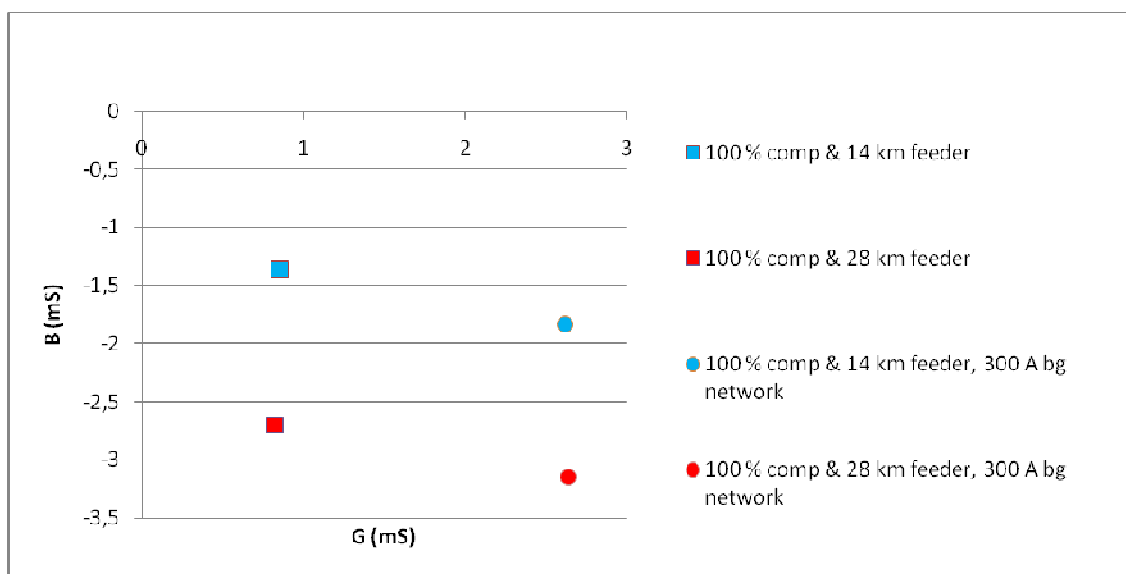


**Figure 63.** Admittance values when background network produces 300 A fault current.

#### 6.6. Odd behaviour of zero sequence current when fault is at the end of the feeder

During the simulations, it was shown that the zero sequence current had odd behavior if the fault is at the end of the studied feeder, and the length of the studied feeder increased. This issue came up during the testing of simulation model. The magnitude

values of zero sequence current  $I_0$  formed a sinusoidal wave as function of length of protected feeder. Three compensation degrees and three background network sizes were simulated and results were always similar. When the background network was larger, sinusoidal wave's amplitude occurred at the shorter feeder length, and when the lowest compensation level was used, the highest point of fault current was reached at longer feeder lengths than with higher compensation levels. At this thesis, this outcome was an extra result and no further investigations were made, but this result has to be taken account if a single feeder length increases to higher lengths than normal. The results are shown in the following three figures.

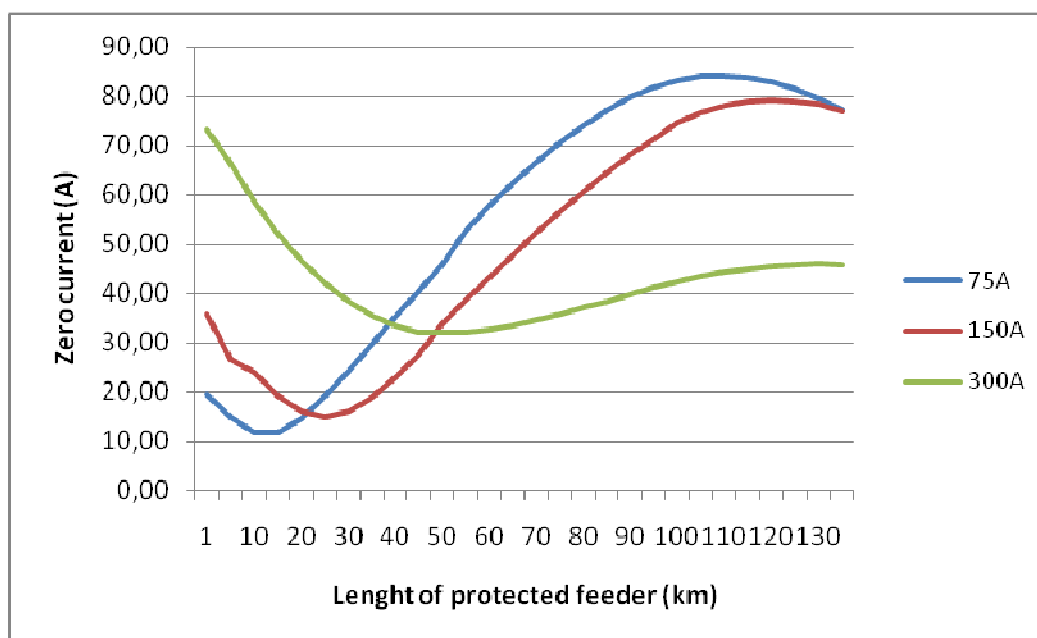


**Figure 64.** Zero sequence current when fault is at the end of the studied feeder and compensation level is 80 %.

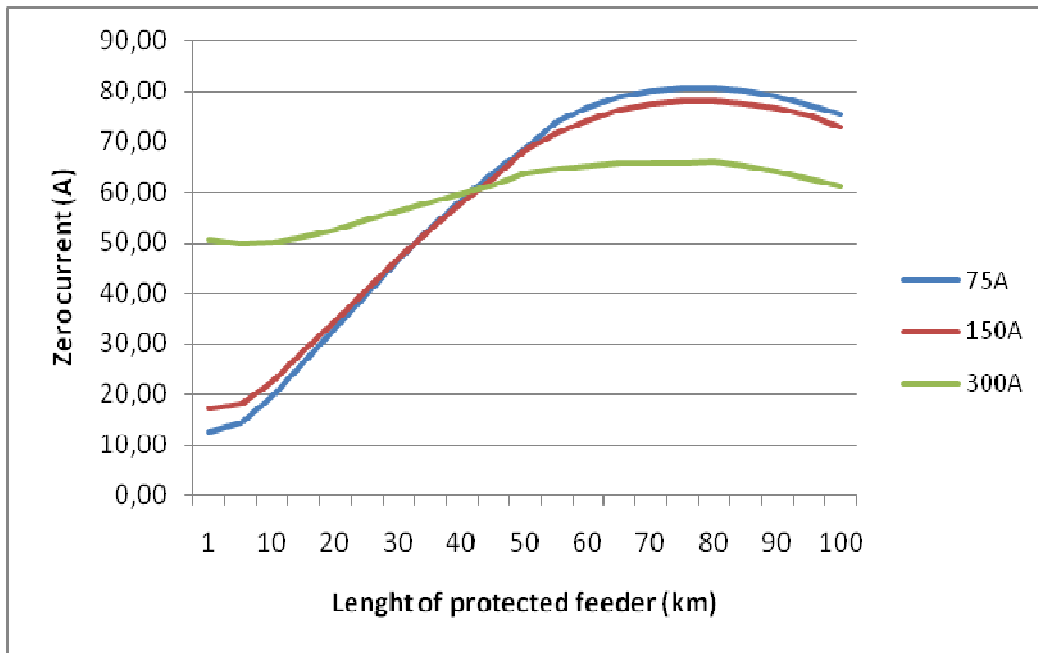


**Figure 65.** Zero sequence current when fault is at the end of the studied feeder and compensation level is 100 %.

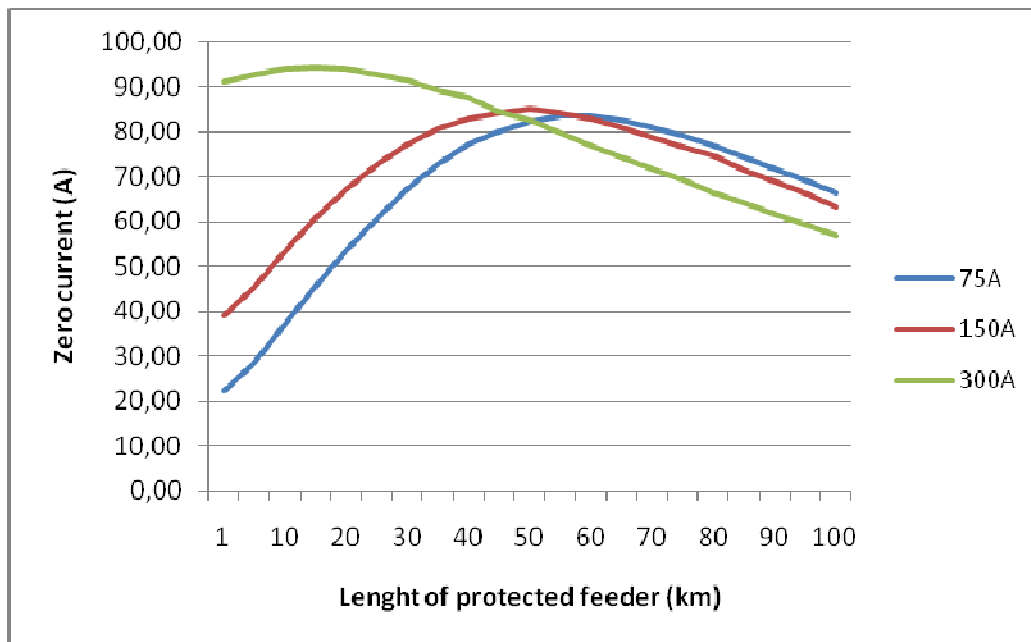


**Figure 66.** Zero sequence current when fault is at the end of the studied feeder and compensation level is 120 %.



## 7. CONCLUSION

From the protection's point of view, all simulations gave promising results. On the one hand, long studied feeder length doesn't cause harm when the simulated protection methods are used, but on the other hand there is no decent solution to lower the resistive current at the actual fault location. No attention was paid to find a solution for that problem, because main focus of this thesis was to test traditional protection methods and their performance. During the simulations, all these functions showed rather good performance. In the ranking, the best method was neutral admittance, then Wattmetric,  $I_{\cos(\varphi)}$ - and base angle criterion. Superiority of the admittance method is explained by its systematical way to identify earth fault and flexibility for different feeder lengths. As an extra result of this thesis was the finding of non-linear behavior of the fault current when the studied feeder length increases to new, never before tested levels. Final analysis of the investigated protection methods are carried out in the following chapters.

### 7.1. Base angle criterion

Base angle measurements showed obvious results. At the voltage measurements, there was significant change in the magnitude when the fault occurs. Some fault location related information could be also acquired. The further at the feeder the fault was, the lower the voltage value was. As mentioned in the results, when the fault occurred at the beginning of the studied feeder, the magnitude of zero sequence voltage  $\underline{U}_0$  was two thirds of network's primary voltage. If the fault resistance was higher than zero, zero sequence voltage was lower. To make earth fault detection more sensitive against high resistance earth faults, Petersen coil's parallel resistance should be added. This increased fault current and by doing so, it also increased magnitude of zero sequence current  $\underline{I}_0$ .

Zero sequence current also showed a clear pattern. When length of the protected feeder increased enough, the magnitude the zero sequence current started to increase too. In every simulated case, highest magnitude of fault current always reached at the longest

length of protected feeder. A clear pattern at resistive part of zero sequence current was also found. When fault occurs further in the studied feeder, resistive fault current decreased in non-linear fashion.

### 7.2. $I_0\cos(\varphi)$ protection method

This protection method utilized the magnitude information of the fault current's resistive part and phase angle difference between residual current and voltage. When the fault was low resistance earth fault,  $I_0\cos(\varphi)$  protection detects faults easily. In the non-fault situation the value was near zero, but when a fault occurred, the value jumped to a magnitude high enough to give secure fault detection. When the fault was a high resistance fault, the measured value decreased as the fault resistance increased. This problem can be avoided by adding a parallel resistor to the Petersen coil. Some decrease at the value was found when background network consisted of 10 feeders instead of 5. The compensation level also had an effect on the  $I_0\cos(\varphi)$  value. The higher the compensation level was, the bigger the non-linear decrease of the resistive fault current was, when the length of the studied feeder increased. This happened only when the fault occurred anywhere else than in the beginning of the studied feeder.

### 7.3. Wattmetric protection method

Wattmetric method also indicated earth faults very well in the simulations. Wattmetric has one drawback when it is compared to  $I_0\cos(\varphi)$  protection. When zero sequence voltage is also taken into account, the further at the feeder the fault was, the smaller the measured value was. When both, current and voltage, decreased, then effect to calculated value was nearly exponential. However this was minor problem, since calculated values are rather high. The same applied to the special case simulation as well, but differences between different studied feeder lengths were bigger.

#### 7.4. Neutral Admittance protection method

Neutral admittance protection showed greatest potential when protection was sought against earth faults. Together with  $\underline{U}_0$  trigger, admittance protection gave perfect results. In all normal simulation cases at the fault situation admittance value could be found from the same quadrant of admittance plane. Special simulations also showed similar results. Even when resistance of fault was 3 k $\Omega$ , it was detected clearly. When fault was in background network, admittance value was in another quadrant than in cases where fault was at the studied feeder. Good protection can be achieved by setting a value for real part of admittance. In cases where the studied feeder length only increases, this setting can be held constant almost every time. This makes this protection method also really flexible.

## REFERENCES

- ABB (1997). *Electrical Transmission and Distribution Reference Book*. 5th ed. United States. ABB Power T&D Company inc.
- ABB (1999). *Protection Application Handbook*. Sweden. ABB Switchgear AB
- ABB (2000). *Technical Specifications and Charts*. 9th ed. Finland. ABB Strömberg ISBN 951-99366-0-2
- ABB (2005). *DEF2 Manual – Directional Earth Fault Protection*. H ed. ABB Distribution automation Ltd.
- ABB (2008). *XLPE Users Guide*. [online]. [cited 2010-03-24]. Available from internet: <url: [http://www05.abb.com/global/scot/scot245.nsf/veritydisplay/62523d62797878abc125720a00285e3a/\\$File/XLPE%20Cable%20Systems%20Users%20Guide%20-%20US.pdf](http://www05.abb.com/global/scot/scot245.nsf/veritydisplay/62523d62797878abc125720a00285e3a/$File/XLPE%20Cable%20Systems%20Users%20Guide%20-%20US.pdf)>.
- Achleitner, G., L. Fickert, C. Obkircher & M. Sakulin (2007). *Reduction of the Net Losses in Distributed Networks*. Clean Electrical Power 2007, Capri, Italy 21-23 May 2007.
- Altonen, Janne & Ari, Wahlroos (2009). *Performance of Novel Neutral Admittance Criterion in MV-feeder Earth-Fault Protection*. 20th International Conference on Electricity Distribution. Prague, Czech Republic 8-11 June 2009.
- Andersson, Lars (2005). *Analysis of System Properties at Increasing Cabling of Medium Voltage Networks*. Engineering thesis. Högskolan Trohättan / Uddevalla. Sweden. 33 p.
- Beaty, H. Wayne (1998). *Electric Power Distribution Systems*. United States. PennWell Publishing Company.

- Berlin, Arne, Hansson Bernt & Olofsson Kristina (2008): *Modulized Distribution Comes to Sweden* [online]. [cited 2010-05-13]. Available from internet: <url:[http://tdworld.com/overhead\\_distribution/modulized\\_distribution\\_comes\\_sweden/](http://tdworld.com/overhead_distribution/modulized_distribution_comes_sweden/)>.
- Carpenter, Guy (2005). *Windstorm Erwin / Gudrun*. [online]. [cited 2010-03-24]. Available from internet: <url:<http://www.dmi.dk/dmi/8januarstormguycarprapport.pdf>>.
- Hakola, Tapio & Matti Lehtonen (1996). *Neutral Earthing and Power System Protection*. Finland. ABB Transmit Oy. ISBN 952-90-7913-3.
- Kothari D.P. & I.J. Nagrath (1994). *Power system engineering*. 7th ed. India. Tata McGraw-Hill Publishing Company Limited. ISBN 0-07-462299-4.
- Kauhaniemi, Kimmo (2007). *Basis of Alternating Current*. [online]. [cited 2010-03-24]. Available from internet: <url:<https://moodle.uwasa.fi/file.php/295/Perusteet.pdf>>.
- Kervinen, Martti & Juhani Smolander (2000). *MAOL Charts, Physics*. 2th ed. Finland. Kustannusyhtiö Otava. ISBN 951-1-16053-2.
- Lakervi, Erkki & Jarmo Partanen (2008). *Electrical Distribution Science*. Finland. Gaudeamus Helsinki University Press. ISBN 978-951-672-357-3.
- Lakervi, Erkki (2006). *Distribution Automation Handbook*. Unpublished. ABB Substation Automation, Vaasa, Finland.
- Lågland, Henry (2004). *Medium Voltage Network Analysis for Modelling*. Master's thesis. University of Vaasa. Finland.
- MATLAB (2010). *MATLAB - The Language Of Technical Computing*. [online]. [cited 2010-03-24]. Available from internet: <url:<http://www.mathworks.com/products/matlab/>>.

PSCAD (2010b). *HVDC - Past, Present & Future*. [online]. [cited 2010-03-24]. Available from internet: <url:https://pscad.com/products/pscad/past\_present\_and\_future/>.

Naver J & R Stilling-Petersen. *Determination of the Supply Quality for Specific Consumers and Ways to Improve this Supply Quality*. [online]. [cited 2010-05-13]. 7 p. Available from Internet: <url:http://ieeexplore.ieee.org/iel3/1185/5893/00225808.pdf?tp=&arnumber=225808&isnumber=5893>.

Nikander, Ari (2002). *Novel Methods for Earth Fault Management in Isolated or Compensated Medium Voltage Electricity Distribution Networks*. Doctor's thesis. Tampere University of Technology. Finland. 200 p.

Pouttu, Jussi-Pekka (2007a). *A Comparison of Earth Fault Protection Methods in Compensated Medium Voltage Networks*. Engineering thesis. University of Applied Sciences of Vaasa. Finland. 89 p.

Pouttu, Jussi-Pekka (2007b). *A Comparison of Earth Fault Protection Methods in Compensated Medium Voltage Networks, Appendix 4*. Engineering thesis. University of Applied Sciences of Vaasa. Finland.

Pouttu, Jussi-Pekka (2007c). *A Comparison of Earth Fault Protection Methods in Compensated Medium Voltage Networks, Appendix 5*. Engineering thesis. University of Applied Sciences of Vaasa. Finland.

Mörsky, Jorma (1993). *Relay Protection Science*. 2th ed. Finland. Otatiето Oy. ISBN 951-672-175-3.

Tobias J C, R P Leeuwerke, A L Brayford & A Rubinson (1998). *The Use of Sectionalizing Circuit Breakers in Urban MV Distribution Networks*. Trends in Distribution Switchgear, IEE Conference Publication No. 459. 7 s. [online]. [cited 2010-04-23]. Available from Internet: <http://ieeexplore.ieee.org/iel4/6003/16052/00744814.pdf?tp=&arnumber=744814&isnumber=16052>.

Tsao T-A & H-C Chang (2003). *Composite Reliability Evaluation Model for Different Types of Distribution Systems*. IEEE Transactions on Power Systems, vol. 18, no. 2. 7 s. [online]. [cited 2010-04-23]. Available from Internet: <http://ieeexplore.ieee.org/iel5/59/26968/01198333.pdf?isNumber=26968&prod=JNL&arnumber=1198333&arSt=+924&ared=+930&arAuthor=Teng-Fa+Tsao%3B+HongChan+Chang>.

Turvatekniikan keskus (2007). *Watch out for Overhead Lines*. [online]. [cited 2010-03-24]. Available from internet: [http://www.tukes.fi/Tiedostot/sahko\\_ja\\_hissit/esitteet\\_ja\\_opaat/Varo\\_ilmajohtoja.pdf](http://www.tukes.fi/Tiedostot/sahko_ja_hissit/esitteet_ja_opaat/Varo_ilmajohtoja.pdf).

Weedy, B.M. (1987). *Electrical Power Systems*. 3rd ed. Great Britain. Bookcraft Ltd. ISBN 0-471-91659-5.

## APPENDICES

## Appendix 1. Matlab® script to import PSCAD results to Matlab®

```

INangledeg = angle(I0dft).*180/pi;
UNangledeg = angle(-U0dft).*180/pi;

Anglediff = UNangledeg - INangledeg;

%Base angle-method

abs_I0dft = abs(I0dft);
abs_U0dft = abs(U0dft);
koko = 1;
step = size(I0dft);
step = step(1);
while koko <= step,
baseangle(koko,1) = angle(I0dft(koko,1));
baseangle(koko,1) = baseangle(koko,1)*180/pi;
koko = koko + 1;
end

%ICOS(phi)-method

angle_rad = Anglediff/180*pi;
cosin = cos(angle_rad);
koko = 1;
step = size(I0dft);
step = step(1);
while koko <= step,
Icosphi(koko,1) = abs_I0dft(koko,1)* cosin(koko,1);
koko = koko + 1;
end

%WattMetric-method

abs_I0dft = abs(I0dft);
abs_U0dft = abs(U0dft);
koko = 1;
step = size(I0dft);
step = step(1);
while koko <= step,
wattmetric(koko,1) = abs_I0dft(koko,1) * abs_U0dft(koko,1) * co-
sin(koko,1) * 1000;
koko = koko + 1;
end

%Admittance-method

koko = 1;
step = size(U0dft);
step = step(1);
while koko <= step,
if U0dft(koko) ~= 0
abs_I0(koko,1) = abs(I0dft(koko,1));

```



```

abs_U0(koko,1) = abs(U0dft(koko,1));
anglerad_I0(koko,1) = angle(I0dft(koko,1));
anglerad_U0(koko,1) = angle(-U0dft(koko,1));
angle_I0(koko,1) = anglerad_I0(koko,1)*180/pi;
angle_U0(koko,1) = anglerad_U0(koko,1)*180/pi;
admittance_abs(koko,1) = abs_I0(koko,1) / (abs_U0(koko,1)*1000);
admittance_angle(koko,1) = angle_I0(koko,1) - angle_U0(koko,1);
else
admittance_abs(koko,1) = 0;
end
koko = koko + 1;
end

%baseangle

baseangle_U_before = abs_U0dft(before,1)*1000;
baseangle_U_after = abs_U0dft(after,1)*1000;
baseangle_U_before
baseangle_U_after

baseangle_I_after = abs_I0dft(after,1);
baseangle_I_after

baseangle_phi_after = baseangle(after,1);
baseangle_phi_after

%icosphi

Icosphi_before = Icosphi(before,1);
Icosphi_after = Icosphi(after,1);
Icosphi_before
Icosphi_after

%wattmetric

wattmetric_before = wattmetric(before,1);
wattmetric_after = wattmetric(after,1);
wattmetric_before
wattmetric_after

%admittance

admittance_abs_before = admittance_abs(before,1)*1000;
admittance_abs_after = admittance_abs(after,1)*1000;
admittance_abs_before
admittance_abs_after

admittance_angle_before = admittance_angle(before,1);
admittance_angle_after = admittance_angle(after,1);
admittance_angle_before
admittance_angle_after

```

## Appendix 2. Data table of PSCAD simulations

All results are shown in four different tables. First three shows results from basic measurements. Each table concentrates on different fault location. When fault is at the beginning of studied feeder number 0 is used. When fault is at the middle point of studied feeder number 0.5 is used. Finally, when fault is at the end of studied feeder number 1 is used. Fourth table concentrates to special case measurements.

Lots of acronyms are used. At the end of acronym “*b*” identifies measurement before fault and “*a*” measurement after the fault. Physical variable identifiers are chosen to identify current and voltage. Acronym “*phi*” identifies angle and “*anglediff*” is faults and current angle difference. “*Abs*” identifies magnitude of value.

**Table 3.** Simulation results when fault is at the beginning of the studied feeder.

km	V	A	deg	A	W	kW	mS	mS	deg	deg	deg
Fault place 0, background network 150 A, fault resistance 0, Compensation degree 80 %, 5 background feeders											
baseangle											
l	u_a	l_a	i_phi_a	icosphi	wattmetric	admittance	abs_b	abs_a	angle_b	angle_a	Anglediff
7	2,825	6332	9,097	-36	0,003500	5,3549	0,009900	33,90	1,4403	1,4368	54
14	1,781	6332	6,679	-53	0,002200	5,3557	0,003900	33,91	1,2534	1,0548	37
28	0,769	6332	6,016	-117	0,000940	5,3571	0,000720	33,92	1,4983	0,9502	-27
56	0,025	6331	17,057	-161	0,000003	5,3594	0,000007	33,93	2,9755	2,6940	-72
Fault place 0, background network 150 A, fault resistance 0, Compensation degree 100 %, 5 background feeders											
baseangle											
l	u_a	l_a	i_phi_a	icosphi	wattmetric	admittance	abs_b	abs_a	angle_b	angle_a	Anglediff
7	4,447	6332	6,964	-120	0,007000	5,3349	0,003130	33,78	1,7250	1,0999	-40
14	3,158	6332	10,179	-148	0,005200	5,3939	0,016400	34,15	2,1254	1,6077	-58
28	1,788	6332	17,886	-163	0,003100	5,2294	0,005500	33,11	3,1814	2,8249	-73
56	0,497	6331	34,305	-171	0,000800	5,3664	0,000400	33,97	5,6096	5,1418	-81
Fault place 0, background network 150 A, fault resistance 0, Compensation degree 120 %, 5 background feeders											
baseangle											
l	u_a	l_a	i_phi_a	icosphi	wattmetric	admittance	abs_b	abs_a	angle_b	angle_a	Anglediff
7	2,556	6332	17,114	-162	0,003500	5,3594	0,008900	33,93	2,6081	2,7030	-72
14	1,610	6332	21,960	-166	0,002200	5,3602	0,003500	33,94	3,3163	3,4689	-76
28	0,679	6332	31,845	-170	0,000900	5,3614	0,000600	33,95	4,8555	5,0296	-80
56	0,019	6331	51,851	-174	0,000024	5,3628	0,000004	33,95	8,0880	8,1895	-84

**Table 4.** Simulation results when fault is at the middle point of the studied feeder.

km	V	A	deg	A	W	kW	mS	mS	deg	deg	deg		
Fault place 0.5, background network 150 A, fault resistance 0, Compensation degree 80 %, 5 background feeders													
baseangle													
l	u_b	u_a	l_a	i_phi_a	b	a	wattmetric	admittance		Anglediff			
								abs_b	abs_a	angle_b	angle_a		
7	2,825	6259	8,947	-37	0,003500	5,2380	0,009900	32,77	1,4409	1,4299	31	54	-54
14	1,780	6183	6,526	-56	0,002200	5,2353	0,003900	32,37	1,2555	1,0555	9	37	-37
28	0,764	6049	5,754	-120	0,000090	5,1252	0,000700	31,00	1,5099	0,9512	-35	-27	27
56	0,019	5686	15,320	-160	0,000002	4,8256	0,000004	27,44	2,9757	2,6945	-65	-72	72
Fault place 0.5, background network 150 A, fault resistance 100 %, 5 background feeders													
baseangle													
l	u_b	u_a	l_a	i_phi_a	b	a	wattmetric	admittance		Anglediff			
								abs_b	abs_a	angle_b	angle_a	Anglediff	
7	4,446	6247	6,860	-129	0,007000	5,2554	0,031300	32,83	1,7448	1,0982	-23	-40	40
14	3,160	6161	9,908	-147	0,005200	5,2505	0,016400	32,35	2,1231	1,6083	-39	-58	58
28	1,787	5956	16,826	-157	0,003100	4,9195	0,005500	29,30	3,1593	2,8254	-57	-73	73
56	0,466	5122	27,753	-154	0,000800	4,3415	0,003000	22,24	5,4865	5,4189	-73	-81	81
Fault place 0.5, background network 150 A, fault resistance 0, Compensation degree 120 %, 5 background feeders													
baseangle													
l	u_b	u_a	l_a	i_phi_a	b	a	wattmetric	admittance		Anglediff			
								abs_b	abs_a	angle_b	angle_a	Anglediff	
7	2,556	6232	16,846	-160	0,003500	5,2752	0,008900	32,88	2,6090	2,7032	-59	-72	72
14	1,609	6115	21,215	-161	0,002200	5,1884	0,003600	31,73	3,3207	3,4693	-66	-76	76
28	0,676	5764	28,996	-158	0,001000	4,8962	0,000600	28,22	4,8758	5,0303	-73	-80	80
56	0,014	4406	36,089	-144	0,000020	3,7476	0,000003	16,51	8,0882	8,1909	-81	-84	84

**Table 5.** Simulation results when fault is at the end of the studied feeder.

km	V	A	deg	A	W	kW	mS	mS	deg	deg	deg
Fault place 1, background network 15 OA, fault resistance 0, Compensation degree 80 %, 5 background feeders											
	baseangle			icosphi		wattmetric		admittance			
l	u_a	l_a	i_phi_a	a	b	a	abs_b	abs_a	angle_b	angle_a	Anglediff
7	2,825	6178	8,879	-39	0,003500	5,2294	0,009900	32,31	1,4411	1,4371	54
14	1,779	6030	6,365	-59	0,002200	5,1063	0,003900	30,79	1,2562	1,0556	-37
28	0,762	5758	5,478	-126	0,000900	4,8798	0,000700	28,10	1,5143	0,9515	-27
56	0,037	5058	13,630	-173	0,000005	4,2980	0,000002	21,74	2,9780	2,6946	-72
Fault place 1, background network 150 A, fault resistance 0, Compensation degree 100 %, 5 background feeders											
	baseangle			icosphi		wattmetric		admittance			
l	u_a	l_a	i_phi_a	a	b	a	abs_b	abs_a	angle_b	angle_a	Anglediff
7	4,446	6138	6,785	-129	0,007000	5,1975	0,031300	31,90	1,7247	1,1008	-40
14	3,161	5998	9,646	-146	0,005200	5,1117	0,016400	30,66	2,1223	1,6084	-58
28	1,787	5601	15,826	-156	0,003100	4,6271	0,005500	25,92	3,1518	2,8255	-73
56	0,447	4184	22,674	-154	0,000700	3,5470	0,000300	14,84	5,4385	5,4187	-81
Fault place 1, background network 150 A, fault resistance 0, Compensation degree 120 %, 5 background feeders											
	baseangle			icosphi		wattmetric		admittance			
l	u_a	l_a	i_phi_a	a	b	a	abs_b	abs_a	angle_b	angle_a	Anglediff
7	2,556	6129	16,569	-158	0,003500	5,1978	0,008900	31,86	2,6090	2,7030	-72
14	1,609	5881	20,404	-157	0,002200	4,9912	0,003600	29,35	3,3221	3,4694	-76
28	0,674	5150	25,904	-151	0,001000	4,3757	0,000600	22,53	4,8813	5,0304	-80
56	0,028	3163	25,900	-141	0,000004	2,6893	0,000010	8,51	8,0897	8,1905	-84

**Table 6.** Special simulations.

km	V	V	A	A	deg	A	W	kW	mS	mS	deg	deg	deg
Fault at background network, background network 150 A, fault resistance 0, Compensation degree 100 %, 5 background feeders													
baseangle													
	u_a	u_b	i_a	i_b	i_phi_a	icosphi	wattmetric	admittance	abs_a	abs_b	angle_a	angle_b	angle_a
14	2,108	6332	8,386	-61	0,003500	-0,2107	0,007300	-1,33	2,1235	1,3240	-39	-91	91
28	0,892	6332	16,695	-65	0,001500	-1,5679	0,001400	-9,93	3,1520	2,6366	-57	-96	96
Fault at background network, background network 150 A, fault resistance 0, Compensation degree 80 %, 5 background feeders													
baseangle													
	u_a	u_b	i_a	i_b	i_phi_a	icosphi	wattmetric	admittance	abs_a	abs_b	angle_a	angle_b	angle_a
14	1,779	6332	8,386	-61	0,002200	-0,2107	0,003900	-1,33	1,2562	1,3244	9	-91	91
28	0,762	6332	16,669	-66	0,000900	-1,5679	0,000700	-9,93	1,5143	2,6366	325	-96	96
Fault place 0.5, background network 150 A, fault resistance 3000 Ω, Compensation degree 100 %, 5 background feeders													
baseangle													
	u_a	u_b	i_a	i_b	i_phi_a	icosphi	wattmetric	admittance	abs_a	abs_b	angle_a	angle_b	angle_a
14	3,160	629	1,059	-143	0,005200	0,6222	0,016400	0,39	2,1231	1,6823	-39	-54	54
28	1,787	523	1,499	-163	0,003100	0,5127	0,005500	0,27	3,1593	2,8658	-57	-70	70
Fault place 0.5, background network 150 A, fault resistance 0, Compensation degree 100 %, 10 background feeders													
baseangle													
	u_a	u_b	i_a	i_b	i_phi_a	icosphi	wattmetric	admittance	abs_a	abs_b	angle_a	angle_b	angle_a
14	3,456	6199	9,317	-153	0,005200	4,0843	0,017900	25,32	1,9905	1,5029	-41	-64	64
28	0,9662	6027	16,643	-161	0,001500	4,0264	0,001500	24,27	3,0492	2,7616	-59	-76	76
Fault place 0.5, background network 300 A, fault resistance 0, Compensation degree 100 %, 5 background feeders													
baseangle													
	u_a	u_b	i_a	i_b	i_phi_a	icosphi	wattmetric	admittance	abs_a	abs_b	angle_a	angle_b	angle_a
14	1,359	5834	18,655	-123	0,005200	15,2813	0,007100	89,15	4,2697	3,1978	-26	-35	35
28	0,839	5369	22,060	-135	0,003300	14,1798	0,002700	76,13	5,0608	4,1090	-39	-50	50
Fault place 0.5, background network 150 A, fault resistance 0, Compensation degree 100 %, 5 background feeders, comp. coil parallel resistance 30 A													
baseangle 1													
	u_a	u_b	i_a	i_b	i_phi_a	icosphi	wattmetric	admittance	abs_a	abs_b	angle_a	angle_b	angle_a
14	2,037	5948	14,420	-123	0,005200	11,9547	0,010700	71,11	2,9079	2,4243	-28	-34	34
28	1,215	5576	18,723	-139	0,003200	11,2677	0,003900	62,83	3,7646	3,3579	-45	-53	53
Fault place 0.5, background network 150 A, fault resistance 0, Compensation degree 80 %, 5 background feeders, comp. coil parallel resistance 30 A													
baseangle 0,8													
	u_a	u_b	i_a	i_b	i_phi_a	icosphi	wattmetric	admittance	abs_a	abs_b	angle_a	angle_b	angle_a
14	1,213	5969	12,523	-75	0,002800	11,9450	0,003400	71,29	2,3431	2,0982	10	17	-17
28	0,543	5652	11,577	-105	0,001300	11,3160	0,000700	63,96	2,4138	2,0481	-16	-12	12